Annu. Rev. Astron. Astrophys. 1989. 27: 555–627

KINEMATICS, CHEMISTRY, AND STRUCTURE OF THE GALAXY

Gerard Gilmore

Institute of Astronomy, University of Cambridge, Madingley Road, Cambridge CB3 0HA, England, and Canadian Institute for Theoretical Astrophysics, University of Toronto, 60 St. George Street, Toronto, Ontario M5S 1A1, Canada

Rosemary F. G. Wyse

Department of Physics and Astronomy, The Johns Hopkins University, Baltimore, Maryland 21218

Konrad Kuijken

Institute of Astronomy, University of Cambridge, Madingley Road, Cambridge CB3 0HA, England, and Canadian Institute for Theoretical Astrophysics, University of Toronto, 60 St. George Street, Toronto, Ontario M5S 1A1, Canada

INTRODUCTION

In principle, an understanding of the formation and early evolution of the Galaxy is a well-defined theoretical problem. All that one requires is a detailed knowledge of the spectrum of perturbations in the early Universe and their subsequent evolution; an understanding of the physics of star formation in a variety of environments, with particular emphasis on a prediction of the distribution of orbital elements of those intermediate-mass massive star binaries that will evolve to supernovae; a description of the hydrodynamics of a protogalaxy, particularly including the effects of a high supernova rate, the efficiency of mixing of the chemically enriched

0066–4146/89/0915–0555$02.00

ejecta, and the incidence of thermal and gravitational instabilities; the growth and transport of angular momentum and their effect on the growth of a disk; and the effects of a time-dependent gravitational potential on the dynamics of any stars formed up to that time. In practice, there remain some limitations in our understanding of at least some of these physical processes. Hence, it is still useful on occasion to try to deduce the important physics involved in galaxy formation from observations of those old stars that were formed at the time of the formation of the Milky Way, and whose present properties contain some fossil record of the Galaxy's history.

The Galaxy offers a unique opportunity to set constraints on theories of galaxy formation and evolution, since only in the Milky Way can one obtain the true three-dimensional stellar spatial density distributions, stellar kinematics, and stellar chemical abundances. Knowledge of how stars move and how they are distributed in space constrains the Galactic potential, while knowledge of their kinematics, ages, and chemistry constrains the star formation history.

We review in Section 1 how the combination of density laws and data on chemical abundances, kinematics, and ages for stars near the Sun provides important information about the early evolution of the Galaxy. Section 2 summarizes some recent results regarding the shape of the stellar distribution in the Galactic spheroid, while Section 3 discusses the importance of observed relations between kinematics and chemistry. We review available data and analyses to show that the sum of all available information strongly suggests that the extreme Population II subdwarf system formed during a short-lived period of dissipative collapse of the proto-Galaxy. This subdwarf system now forms a flattened, pressure-supported distribution with axial ratio $\sim 2:1$. Section 4 is devoted to the nature and evolutionary status of the thick disk, which formed subsequent to the subdwarf system, with at least the metal-poor tail of the thick disk being comparable in age to the globular cluster system. The thick disk is probably chemically and kinematically discrete from the Galactic old disk, though the data remain inadequate for robust conclusions. The final section (Section 5) reviews the status of "missing" matter in the thin disk; new data and analyses lead to the conclusion that there is no statistically significant amount of nonluminous mass in the solar neighborhood and hence no evidence for dissipative dark matter.

1. THE FORMATION OF DISK GALAXIES

Current understanding of the formation and early evolution of disk galaxies allows a description of the important physical processes at various levels of complexity and generality. At one extreme, one simply considers

the global evolution of a gas cloud and assumes that mean values of relevant parameters suffice for an adequate description of generic properties. Alternatively, one gives up general applicability, adopts instead specific numerical values for those parameters that quantify the important physics, and attempts a detailed confrontation of model predictions with observed stellar populations. The relation of any model prediction to detailed observations at a single radius in a specific galaxy clearly needs to be considered with some care. Mindful of this caveat, we outline here the most important time scales and physical processes that are likely to play a role in the determination of the observable properties of galaxies like the Milky Way.

1.1 *Dissipational Disk Galaxy Formation*

The existence of cold, thin, galactic disks has strong implications for galaxy formation. To see this, consider a standard picture whereby galaxies form from growing primordial density perturbations, which expand with the background universe until their self-gravity becomes dominant and they collapse upon themselves. Were there to be no loss of energy in the collapse, and if we neglect angular momentum, the transformation of potential energy into thermal (kinetic) energy would lead to an equilibrium system with final radius equal to half its size at maximum expansion, supported by random motions of the constituent particles. Thus an equilibrium, purely gaseous protogalaxy should have temperature

$$T \equiv T_{\rm virial} \sim \frac{GMm_{\rm p}}{kR}, \qquad 1a.$$

and a stellar protogalaxy should equivalently have velocity dispersion

$$\sigma^2 \sim T_{\rm virial} \frac{k}{m_{\rm p}}, \qquad 1b.$$

where k and $m_{\rm p}$ are the Boltzmann constant and mass of the proton, respectively. Numerically, we have $T_{\rm virial} \sim 10^6 R_{50}^{-1} M_{12}$ K for gravitational (half-mass) radius R, in units of 50 kpc, and mass M, in units of $10^{12}\ M_\odot$. Since the disks of spiral galaxies are cold with $T \ll T_{\rm virial}$, energy must have been lost. Since this lost energy was in random motions of individual particles, the only possible loss mechanism is through an inelastic collision, leading to the internal excitation of the particles and to subsequent energy loss through radiative deexcitation. Clearly, particles with small cross section per unit mass for collisions, such as stars, will not dissipate their random kinetic energy efficiently, and thus dissipation must occur prior to star formation, while the galaxy is still gaseous. The virial temperature

of a typical galactic-sized potential well is $T_{\rm galaxy} \sim 10^6$ K, with corresponding one-dimensional velocity dispersion of ~ 100 km s^{-1}.

The physical conditions of the Universe at the epoch of galaxy formation ($z \sim$ a few), as deduced from observations of quasar absorption lines (the Gunn-Peterson test for neutral hydrogen), are such that hydrogen is ionized and the temperature of the protogalactic gas is $\sim 10^4$ K, with a sound speed of only ~ 10 km s^{-1}. Thus, collapse of this gas in galactic potential wells will induce supersonic motions and lead to both thermalization of energy through radiative shocks and subsequent loss of energy by cooling. It is this conversion of potential energy—first to random kinetic energy as described by the virial theorem and then to radiation via atomic processes, the net result of which is an increase in binding energy of the system—that is termed dissipation.

The rate at which excited atoms can cool is obviously a fundamental limit on the amount and rate of dissipational energy loss and hence on the maximum rate at which a gas cloud can radiate its pressure support and collapse. A convenient measure of this time scale is the *cooling time* of a gas cloud, which is the time for radiative processes to remove the internal energy of the cloud. Defining the cooling rate per unit volume to be $n^2\Lambda(T)$ (where n is the particle number density, and where the functional form of Λ is determined by the relative importances of free-free, bound-free, and bound-bound transitions and thus is an implicit function of the chemical abundance) gives

$$t_{\rm cool} = \frac{3nkT}{n^2\Lambda(T)} \propto \frac{T}{n\Lambda}. \qquad 2.$$

It is usually of most interest to compare this time scale with the global *gravitational free-fall collapse time* of a system, which is the time it would take for the system to collapse upon itself if there were no pressure support. This time scale depends upon only the mean density of the system and is given by

$$t_{\rm ff} \sim 2 \times 10^7 n^{-1/2} \text{ yr}. \qquad 3.$$

The term *rapid* is often used to describe evolution that occurs on about a free-fall time.

An example of the role of atomic processes in allowing dissipation and increase of binding energy during galaxy formation, which though idealized is still of interest in comparisons with observation, was discussed in three contemporaneous papers—Rees & Ostriker (1977), Binney (1977), and Silk (1977), following the earlier work of Lynden-Bell (1967a). These authors investigated the nonlinear (collapse-phase) evolution of (baryonic)

cosmological density perturbations in the density-temperature plane. [These ideas are straightforwardly adapted to allow for a significant non-baryonic component of galaxies (see e.g. White & Rees 1978, Fall & Efstathiou 1980, Blumenthal et al. 1984).] In the Rees & Ostriker model, the perturbation is hypothesized to be initially sufficiently lumpy and chaotic that collisions between local irregularities lead to efficient shock thermalization of the kinetic energy of collapse, resulting in a hot ($T \sim T_{\rm virial} \sim 10^6$ K), pressure-supported system. The subsequent evolution will then depend on the efficiency with which the heated gas can radiate, and it can be calculated readily if one assumes for simplicity that the system is also of uniform density. (These simplifying assumptions, of course, remove the possibility of any useful discussion of star formation, which depends on *local* cooling and instability, in this model.) One may then define a curve in the density-temperature plane where the gas-cooling time equals the free-fall collapse time of the perturbation itself. Systems that formed with a *short* cooling time will occupy a locus inside this curve. The $t_{\rm cool} = t_{\rm ff}$ locus has an upper boundary corresponding to $M \sim 10^{12}\ M_\odot$, $R \sim 100$ kpc; the fact that these limits also correspond to the upper bound of masses and radii characteristic of observed galaxies is very suggestive. Indeed, when one translates observed surface brightnesses and velocity dispersions of galaxies to put them on the density-temperature plane, one finds that present-day galaxies of all Hubble types lie within the $t_{\rm cool} = t_{\rm ff}$ curve, whereas groups and clusters of galaxies lie outside (Silk 1983, Blumenthal et al. 1984). This can be interpreted to imply that the luminous parts of galaxies cooled and collapsed rapidly, at least for those galaxies of high enough central surface brightness to have been studied to date (see Disney 1976, Bothun et al. 1987). Indeed, Gunn (1982) finds that the "bulge" of the Milky Way individually also lies within the $t_{\rm cool} \lesssim t_{\rm ff}$ locus of the density-temperature plane, which suggests that it too dissipated on a time scale comparable to its free-fall collapse time. We defer discussion of the other observational constraints on the duration of the formation of the metal-poor spheroid of the Milky Way to Section 3 below.

The evolution of very massive ($M \gtrsim 10^{12}\ M_\odot$) protogalaxies is, however, only poorly determined by this theory. These galaxies may have had an early pressure-supported, quasi-static collapse phase, provided, of course, that the cooling time is less than the Hubble time; such density perturbations may plausibly evolve along a constant Jeans'-mass track (with density and temperature increasing and little or no star formation) in the density-temperature plane, until conditions are such that the cooling time is less than the dynamical time and rapid collapse is again expected to ensue. An alternative to this last conjecture was suggested by Fall & Rees (1985), who argued instead that conditions within a protogalaxy, once the

global cooling and collapse times became comparable, may lead to thermal instability, with a background plasma of temperature $T \sim T_{\rm virial} \sim 10^6$ K and embedded, dense condensations of temperature $T \sim 10^4$ K. The important mass scale of the condensations is still set by gravitational instability, however.[1] Regardless of the fine-tuning required in theories of the formation of globular clusters, the basic idea that thermal instability might cause a sufficiently massive protogalaxy to "hang up" with $t_{\rm cool} \gtrsim t_{\rm ff}$ in its early stages of evolution suggests that the spheroids of at least very massive galaxies may have collapsed less rapidly than on a free-fall time, with continuing star formation in thermally unstable condensations perhaps being possible over this longer time.

The discussion above is based on an extremely idealized model of a protogalaxy, in that only the *global* cooling and collapse time scales of a *uniform* gas cloud are considered. No analytic descriptions of more plausible models exist as yet. A first step has been made by White (1989a), who considers an idealized, spherically symmetric gas cloud that has an imposed initial density gradient. White's models are motivated by cosmologies dominated by cold dark matter (CDM) and assume that 90% of a galaxy is nonbaryonic, and that the remaining 10% is gas that is initially distributed in proportion to the total density, which has a profile consistent with observed flat rotation curves. The inner, more dense regions then cool on a shorter time scale than the outer regions, so that one can define a time-dependent "cooling radius" for each protogalaxy within which the gas is sufficiently dense to cool on a Hubble time. What happens to the gas within the cooling radius is as indeterminate in this model as in those discussed above. However, one can imagine earlier and slower star formation in the central regions than the previous models suggested.

The above discussion can say nothing about when or how local Jeans'-mass condensations actually form stars; the inherent assumption is that cooling is necessary and sufficient for efficient star formation, though the critical distinction between global and local time scales is rarely made explicit. However, it is clear that the existence of *gaseous* disks requires

[1] Fall & Rees suggest that this phase of galactic evolution represents an epoch of globular cluster formation, since the Jeans' mass under these conditions is $\sim 10^6\, M_\odot$. (The *Jeans' mass* is that minimum mass at which gravity overwhelms pressure, so that density perturbations of mass $M \gtrsim M_J \sim 10^8 T_4^{3/2} n^{-1/2}\, M_\odot$ are unstable and collapse upon themselves, where the numerical factor is for temperature T, in units of 10^4 K, and number density n, in units of particles cm^{-3}.) However, the Jeans' mass will be continually reduced, presumably to stellar masses, unless further cooling by molecular hydrogen is suppressed in some way. Thus, continuing formation of globular cluster–sized objects requires some additional special conditions.

that the star-formation efficiency be low during the early stages of disk formation. A realistic discussion of galaxy formation must consider the hydrodynamics of the gas in a protogalaxy. Numerical computation of hydrodynamic models of galaxy formation can contain an explicit formulation of the rate of star formation, along with the other important time scales of gaseous dissipation, viscous transport of angular momentum, and free-fall collapse. Larson's (1976) models still offer the most detailed discussion of the effects of gas processes within the prescription of galaxy formation, despite the limitations imposed by his computational constraints. These models identify the major requirements for producing galaxies that contain *both* a high-central-surface-brightness, nonrotating stellar spheroid and an extended, cold, gas-rich disk—initially both the star formation rate and viscosity must be high to form the nonrotating but centrally concentrated stellar spheroid, but both these quantities must be suppressed later to form a thin, lower central surface density, centrifugally supported, gas-rich disk. Carlberg (1985) has pioneered the "sticky particle," modified N-body approach, and several groups have initiated studies of disk galaxy evolution using the smoothed-particle hydrodynamics (SPH) scheme. The general conclusion from available studies is that, while it is possible to build models that are somewhat like observations, it is necessary to specify the most sensitive parameters (viscosity and, in effect, the star formation rate) in an ad hoc way. Considerably more sophisticated numerical experiments are required to ensure a plausible treatment of the hydrodynamics of a multiphase interstellar gas in a system with a high supernova rate, even under the assumption that one understood how to parameterize viscosity and star formation and knew the initial conditions.

An important general feature of recent models of disk galaxy formation is exemplified by Gunn's (1982) continual-infall models. These models hinge on the existence of loosely bound material surrounding a density peak whose central regions are collapsing (rapidly) to form a galaxy; they are extensions of the cosmological secondary-infall paradigm of Gunn & Gott (1972), modified to include dissipation of the infalling gas. The free-fall collapse time scales for the outer regions can be of order a Hubble time, leading to a picture of disk galaxy formation whereby the central regions collapse rapidly to form the bulge, followed by accretion of proto-disk material. In so far as the subsequent evolution of the gas may be modeled through the processes of shock heating, cooling, and star formation, the general features of continual-infall models are in good qualitative agreement with observed galactic disks. Thus one might reasonably expect that galactic *disks* formed on a longer time scale, though still without pressure support having played a major role, than did galactic spheroids,

the slower collapse of disks being due simply to their lower density initial conditions implying a longer free-fall collapse time. The lack of disk-dominated systems in dense environments such as rich clusters of galaxies is consistent with this picture of unperturbed, continual accretion of disks (Larson et al. 1980, Frenk et al. 1985).

The angular momenta of galaxies that formed in environments of different density might also be expected to differ. The specific angular momentum distribution of the material surrounding density peaks has been investigated analytically by Ryden (1988) in the context of cold dark matter–dominated cosmological models, and by Barnes & Efstathiou (1987), using N-body techniques, for various assumed cosmological power spectra. The consensus is that the effect of tidal torques is to produce a system with specific angular momentum increasing with radius. Zurek et al. (1988) and Frenk et al. (1988) have shown that in CDM, or any scenario where chaotic aggregation of smaller systems is part of the formation of galaxy-sized systems, dynamical friction of dense clumps on the smoother background causes transport of both energy and angular momentum from the orbiting clumps to the smooth outer regions. Thus, during the buildup of structure, initially strongly bound particles lose both energy and angular momentum, whereas the weakly bound particles gain energy (become more weakly bound) and also gain angular momentum. There is overall alignment of the angular momentum vector of different shells in binding energy. These authors argue that slowly rotating stellar systems, such as giant elliptical galaxies or spheroids of disk galaxies, form in direct analogy to the dissipationless dark halos that they model (i.e. with lots of dynamical friction and merging of stellar clumps, the dark halo and outer stellar envelope taking up the angular momentum transported outward). Disks of spiral galaxies would then form without significant angular momentum transport, owing to the expectation that the baryons remain gaseous until the virialization of the dark halo, and shock heating (as described earlier) would homogenize the gas. The predictions of these models could be tested in detail if we knew the angular momentum distribution of the outer spheroid of our Galaxy; all we know at present is that the *kinematically selected* subdwarfs in the solar neighborhood have a lower specific angular momentum than do the disk stars, by roughly a factor of five, and that the metal-poor globular cluster system is consistent with zero net rotation to Galactocentric distances of ~ 30 kpc.

The angular momentum distribution of the material destined to form the disk controls both the range of galactocentric radii over which infall occurs at a given epoch and the duration of the infall at a given location. Thus, models of disk chemical and dynamical evolution that appeal to continual infall must also satisfy angular momentum constraints.

1.2 *Specific Models of Milky Way Galaxy Formation*

The most widely referenced model of the formation of our Galaxy is that of Eggen et al. (1962; henceforth ELS), which was developed primarily to understand their observations of the kinematics and chemical abundances of stars near the Sun. This model requires that the stellar spheroid formed during a period of rapid collapse of the entire proto-Galaxy, subsequent to which the remaining gas quickly dissipated into a metal-enriched cold disk, in which star formation has continued until the present. The ELS model was designed to provide conditions under which the oldest stars populated radially anisotropic orbits, whereas stars that formed later had increasingly circular orbits, in accord with their data, which implied that the most metal-poor stars (assumed to be the oldest stars) were on more eccentric, lower angular momentum orbits than were the more metal-rich stars. This model is based on two crucial assumptions. The first is that a pressure-supported, primarily gaseous galaxy (where $T = T_{\text{virial}}$) is stable against star formation. In this case, the *global* cooling time is the shortest time scale of interest, and thermal instabilities of the type invoked by Fall & Rees (1985) and discussed briefly above must be suppressed. The second assumption is that stellar orbits cannot be modified to become more radial after formation of the star.

If the first assumption is valid, the observed high-velocity stars must have formed from gas clouds that were not in equilibrium in a pressure-supported system. If the second assumption is valid, these clouds formed stars while on radial orbits at large distances from the Galactic center. Thus in this picture, these clouds must have turned around from the background universal expansion and be collapsing toward the center of the potential well. Hence, the oldest stars of the Galactic spheroid must have formed as the proto-Galaxy coalesced. To determine the *rate* of the collapse, ELS analyzed the evolution of the radial anisotropy of a stellar (or gas cloud) orbit as the Galactic potential changed and showed that it was approximately conserved during a slow collapse, but that it became more radially anisotropic in a fast collapse. They argued against a slow collapse on the grounds that such a collapse requires tangentially biased velocities (recall that pressure support has been excluded by assumption), and this tangential bias will be unaffected by the resulting slow changes of the gravitational potential. The observed radial anisotropy of the stellar orbits then implies an initially radially biased velocity ellipsoid, while the calculations of ELS show that such a velocity ellipsoid will have become more radially anisotropic during collapse. Hence, ELS deduced that the gas clouds were in free-fall radial orbits, and that the consequent collapse must have been rapid, "rapid" in this sense meaning that the time scale

for collapse is comparable to an orbital or a dynamical time scale, which is a few $\times 10^8$ yr. It should be noted that Isobe (1974) came to the opposite conclusion from his analysis of the ELS data and favored a slow collapse, while Yoshii & Saio (1979) augmented the ELS sample and also concluded that the halo collapsed over many dynamical times. We return to the difficulty of inferring a time scale in Section 3 below.

Clearly, if either of ELS's assumptions were violated, there need be no correlation between the *time* of a star's formation—which they infer from a star's metallicity—and its *present* orbital properties. In a nonrotating, pressure-supported system, all stars formed would be on highly radial orbits, as the star has too small a surface area to be pressure supported by the gas. As we mentioned above, assumptions about star formation in pressure-supported systems must be treated as ad hoc until we understand better the physics of star formation, so that conclusions based on such assumptions are at best uncertain. If their second assumption were violated, then the stars that are now the high-velocity stars near the Sun could have originated from more circular orbits interior to the Sun and have present orbital properties that depend only on dynamical processes subsequent to their formation. The realization that a forming galaxy undergoes changes in its gravitational potential that are of order the potential itself (violent relaxation) means that stellar orbits can be modified considerably.

Recent *N*-body models [see, for example, May & van Albada (1984) and McGlynn (1984) for excellent descriptions of representative experiments] for systems in which dissipation does not play a major role show that the final state of the collapsed system depends on both the degree of homogeneity and on the temperature of the initial state. As seen in the cosmological *N*-body simulations discussed above, clumps cause angular momentum and energy transport. Violent relaxation never goes to completion, so that final and initial orbital binding energies and angular momenta are correlated, with the interior regions becoming more centrally concentrated and the outer regions being puffed up. The typical final steady-state velocity distribution is highly anisotropic exterior to (roughly) the half-light radius and more isotropic interior to that radius. If violent relaxation were completely efficient, all systems would reach the same final state with isotropic velocity distribution. In the Galaxy, the spheroidal half-light radius is ~ 3 kpc, well interior to the Sun's orbit. Thus the expected velocity distribution of old stars near the Sun after virialization of the spheroid is anisotropic, as observed by ELS, even though the dynamical evolution of the system is not as they envisage and a correlation between kinematics and age is no longer an inevitable conclusion. One might, for example, imagine a situation where later (rapid) collapse of

either the disk or the dark halo, or the merger of a few large substructures, could lead to rapid dynamical evolution of a central spheroidal component that had previously formed on a longer time scale. Models of this type have yet to be studied in detail.

The implications of the ELS model and the current status of the relevant observational correlations are discussed more fully in Section 3.2 below.

1.3 *The Time Scales of Galactic Chemical Evolution*

In attempting to deduce the rate of star formation and dynamical evolution in a proto-galaxy, it is desirable to have available a clock whose rate can be calibrated independently of the naive discussions of global gas cloud properties noted above, and that runs sufficiently quickly to resolve the dynamical evolutionary time scales. Such a clock is provided by stellar evolution of high-mass stars, while the fossil record of the clock is observable in the chemical abundance enrichment patterns in long-lived low-mass stars. Fortunately, there exists a subset of common elements (most importantly oxygen) whose creation sites are restricted to very massive stars, and another subset (most importantly iron) that is created also during the evolution of lower mass stars (in merging-binary supernovae). Since the evolutionary time scales for high- and low-mass stars span the time-scale range of interest in galaxy formation, the differential enrichment of oxygen and iron provides an ideal clock to calibrate the rate of star formation in the proto-Galaxy.

Oxygen-to-iron element ratios have now been measured for a sufficient number of stars to define the systematic trends in the data. The observations are well reviewed by Wheeler et al. (1989) in this volume and are not discussed further here. The important result for present purposes is that a significant change of slope occurs in the relationship between the element ratio [O/Fe] and [Fe/H] (a similar relationship holds for [α/Fe], where the "alpha" elements are those synthesized by successive capture of alpha particles, such as Mg, Si, Ca, and Ti) close to metallicities where there also occurs a change in the stellar kinematics—that is, at [Fe/H] ~ -1([O/Fe], [α/Fe]) and ~ -0.4([α/Fe]), although the latter break is less well established. The [O/Fe] ratio is observed to be approximately constant, independent of [Fe/H] for the most metal-poor stars ($-2.5 \lesssim$ [Fe/H] $\lesssim -1$), while [O/Fe] declines for the more metal-rich stars ([O/Fe] $\sim -1/2$ [Fe/H]). Present data are summarized in Figure 1, in which all scatter is considered by the relevant observers to be consistent with observational error, i.e. there is *no* cosmic scatter (see also Wheeler et al. 1989). If we assume that [Fe/H] is a monotonically increasing function of time, the mean trend in the figure can be explained if the oxygen and iron in the more metal-poor stars have been produced in (massive) stars of the

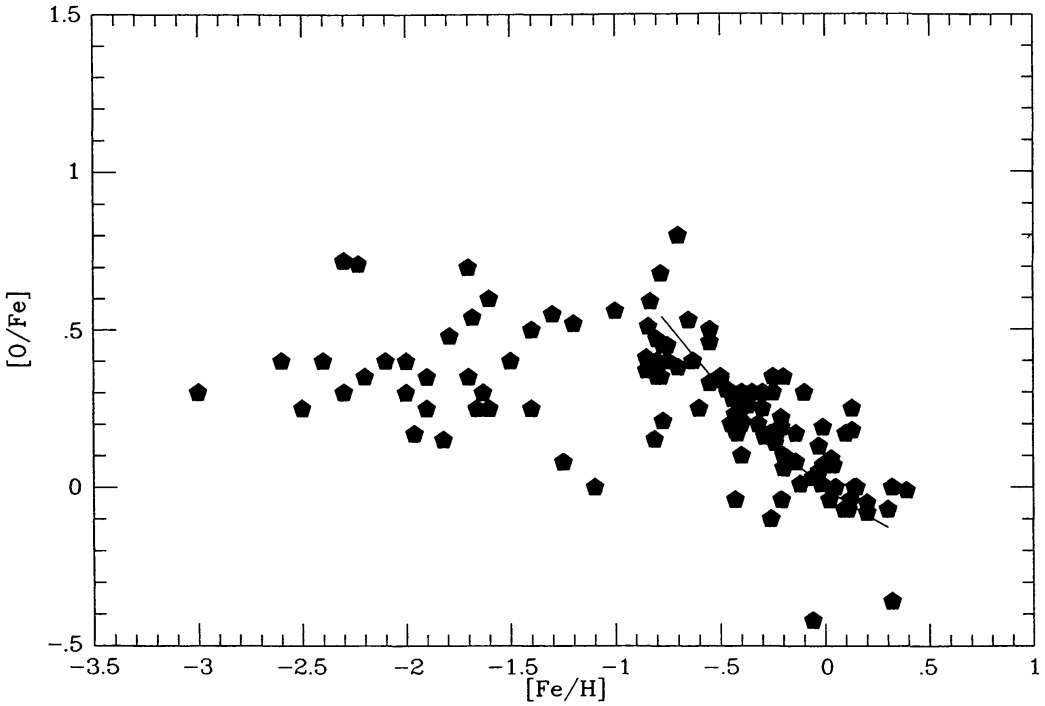

Figure 1 A compilation of oxygen to iron element ratio measurements from the literature and from B. Barbuy (private communication; her [O/Fe] values derived from the near-IR line have been offset by 0.2 dex for internal consistency). This figure is adapted from Wyse & Gilmore (1988). The smooth curve through the data for [Fe/H] $\gtrsim -1$ shows the prediction of a simple model with constant supernova rates in the ratio 1.5:1.0 for Type I:Type II, which results in twice as much oxygen as iron being produced per unit time (see Section 3.4).

same (short) lifetime, whereas for the more metal-rich stars, although the oxygen and iron continue to be produced together, an additional, longer time scale source now dominates the iron production. Such behavior is in good agreement with supernova nucleosynthesis calculations, which show that oxygen is produced only in Type II supernovae by massive stars ($M \gtrsim 20\ M_\odot$), while iron has a contribution from both massive and low-mass stars ($M \gtrsim 3\ M_\odot$, Type I supernovae) and thereby has an enhanced production once the much more numerous, lower mass stars contribute to its nucleosynthetic yield (Tinsley 1979, Matteucci & Greggio 1986). This results in the ratio [O/Fe] decreasing systematically with increasing metallicity [Fe/H]. The main-sequence lifetimes τ_{ms} of single stars of masses 0.08 $M_\odot$ to 100 $M_\odot$ can conveniently be estimated from the following (P. P. Eggleton, private communication):

$$\tau_{ms} = \frac{2.5 \times 10^3 + 6.7 \times 10^2 M^{2.5} + M^{4.5}}{3.3 \times 10^{-2} M^{1.5} + 3.5 \times 10^{-1} M^{4.5}} \text{ Myr.} \qquad 4.$$

The main-sequence lifetime of massive stars approximates the time scale

for oxygen enrichment, while the main-sequence lifetime of the stars responsible for Type I supernova explosions provides a lower limit to the time scale of "secondary" iron production.

In terms of models of the early chemical evolution of the Galaxy, one must explain why [O/Fe] is approximately constant, at three times the solar value, for [Fe/H] $\lesssim -1$, but decreases smoothly for [Fe/H] greater than this value, as well as why the mass of stars with [Fe/H] $\lesssim -1$ is only a few percent of the total stellar mass of the Galaxy, as discussed in detail in Section 4. Clearly, the approximate constancy of the [O/Fe] ratio independent of the [Fe/H] ratio at low metallicities requires that essentially *all* the stars with [Fe/H] $\lesssim -1$ formed on a time scale less than that on which a significant number of low-mass (Type I) supernovae exploded. This time scale is rather difficult to estimate precisely, owing to uncertainties in the mechanism of Type I supernovae and the fraction of all stars formed that are in binaries of the type that may be expected to be precursors (cf. Iben 1986); the lowest mass, and hence most numerous, progenitors of CO white dwarfs have main-sequence masses and lifetimes of $\sim 5\ M_\odot$ and $\sim 2.5 \times 10^8$ yr, respectively. Thus a reasonable estimate for the characteristic time after which one expects dominance of iron from Type I supernovae is $\lesssim 10^9$ yr (but bear in mind that some Type I systems will take a Hubble time to evolve). This general argument appears to be the strongest direct evidence for a rapid formation time scale for the extreme Population II stars in the Galaxy and is in agreement with the (currently more contentious) kinematic evidence discussed below (Section 3). It follows from this that a straightforward test of the formation time scale of the metal-rich central bulge would be to measure the [O/Fe] values for some metal-rich stars and compare them with those of corresponding field stars. For a constant IMF, if the oxygen is overabundant then the bulge must have formed on the same time scale as that of the metal-poor spheroid (i.e. rapidly and long ago), and vice versa if the oxygen is not overabundant.

This relatively short time scale for spheroid evolution to [Fe/H] ~ -1 may be compared with that inferred from the evolution of *r*- and *s*-process nucleosynthesis. Gilroy et al. (1988) find no evidence for the *s*-process from the heavy-element abundance in very metal-poor giants ([Fe/H] $\lesssim -2$), which implies that the time scale for this level of iron enrichment was shorter than that involved in nucleosynthesis via the *s*-process. Details of the *s*- and *r*-process sites and production mechanisms are not well understood, but it is generally thought that *s*-process isotopes are produced during helium shell flashes (thermal pulses) in intermediate-mass stars ($2 \lesssim M/M_\odot \lesssim 8$) on the asymptotic giant branch, with subsequent mixing (dredge-up) bringing these to the surface, where they are lost in a stellar

wind (cf. Iben 1985). The *r*-process probably occurs during Type II supernovae. The lifetimes given by Equation 4 lead to the conclusion that the Galaxy had enriched to [Fe/H] ~ -2 in $\lesssim 10^8$ yr (cf. Gilroy et al. 1988). A further important finding of Gilroy et al. is that there *is* cosmic scatter in the relative abundances of *r*-process elements in these very metal-poor stars, in that stars of the same [Fe/H] show large variations in, for example, [Eu/Fe]. This contrasts with the apparent lack of cosmic scatter in other element ratios, such as oxygen. This is plausibly a manifestation of the inhomogeneity of the early spheroid; it should be remembered that the mass fraction of the metal-poor spheroid with [Fe/H] $\lesssim -2$ dex is $\lesssim 20\%$, adopting a mean metallicity of -1.5 dex and dispersion $\sigma_{[Fe/H]} \sim 0.5$ dex (Gilmore & Wyse 1985, Laird et al. 1988b). This corresponds to at most a few percent of the total stellar mass of the Galaxy, so that one expects local fluctuations in heavy-element enrichment due simply to Poisson noise in the very small number of supernovae that can have exploded at that stage of the Galaxy's evolution. This argument predicts that comparable inhomogeneities will be observed in all element ratios for stars with [Fe/H] $\lesssim -2$.

If the arguments above concerning the production time scales of different elements contained the whole story of chemical enrichment over the history of star formation in the Galaxy, then it would have to be mere coincidence that the change in the predominant production mechanism of iron occurred close to a metallicity, or epoch, at which the stellar kinematics change from those of a pressure-supported system (which formed stars rapidly) to those of an angular momentum–supported system. Rather, the coincidence of the value of [Fe/H] at which the Galaxy changed from a pressure-supported system to an angular momentum–supported system with the value of [Fe/H] at which the interstellar medium first became diluted by the products of long-lived stars provides a diagnostic of the relative star formation and dissipation rates in the proto-Galaxy.

One may limit the maximum allowed variations in the star formation rate by making the conservative assumption that the (2σ) scatter about the mean trend in [O/Fe] against [Fe/H] of a few tenths of a dex, or about a factor of two, reflects real cosmic scatter, rather than measurement uncertainties, even though all the observed scatter is consistent with measurement uncertainties. The number of Type I supernovae at a given time is determined by the star formation rate some 10^9–10^{10} yr previously, while that of Type II supernovae is determined by the star formation rate at that time. The scatter would then be caused by short-lived increases in the star formation rate leading to enhanced rates of Type II supernovae. Scatter of a factor of two implies that the Type II formation rate be increased by a factor of $\lesssim 4$ for a 2σ effect. Hence the mean star formation

rate in the Galaxy cannot have increased by a factor of 4 since the Galaxy attained a metallicity of -1 dex. The average star formation rate during the formation of the low-mass, metal-poor spheroid was $\sim 10\ M_\odot\ \mathrm{yr}^{-1}$, which is of the order of a typical present-day disk star formation rate. Thus disk galaxies, by far the most common nondwarf galaxies in the Universe, do not go through a sustained, highly luminous burst of star formation in their earliest stages and are not good candidates for detection in primeval galaxy searches.

When sufficient data and reliable massive-star evolutionary models all the way through the supernova explosion, with corresponding elemental yields, become available, it will be possible to quantify these arguments (subject to the assumption of a constant stellar initial-mass function) and provide a real time scale (in years) for the periods of protogalactic evolution that were dominated by collapse (possibly nondissipational) on a dynamical time scale, and for that period when angular momentum support became the dominant dynamical process.

One conclusion that is relatively independent of the details of elemental synthesis follows from the fact that features in both the stellar abundance and kinematics occur more or less together at $[\mathrm{Fe/H}] \lesssim -1$. A discontinuity in kinematic properties implies that the ratio of the dissipation rate to the star formation rate changes rapidly. A possible explanation is that at metallicities $[\mathrm{Fe/H}] \gtrsim -1.5$, the efficiency with which a gas cloud cools from $\sim 10^6$ K (a typical galactic virial temperature) increases markedly owing to a transition of the dominant cooling mechanism from free-free radiation (independent of metallicity) to line radiation (proportional to the number density of metals). Thus a rapid increase in the dissipation rate and collapse to a disklike angular momentum–supported structure is not implausible at a metallicity of ~ -1 dex. It is not crucial for these arguments that the breaks in kinematics and element ratios occur at *exactly* the same metallicity.

2. THE SPATIAL STRUCTURE OF THE MILKY WAY GALAXY

Counting stars is one of the few truly classical scientific techniques used to study high-latitude (and therefore low-obscuration) Galactic structure. The extensive data set and understanding available in 1965 are reviewed in many excellent articles in Volume 5 of the "Stars and Stellar Systems" series (Blaauw & Schmidt 1965). Relatively little further progress was achieved until the new deep high-quality data of I. R. King and collaborators at Berkeley became available in the late 1970s. The application of computer modeling to these data by van den Bergh (1979) led to a

considerable resurgence of interest, continuing to the present. Recent relevant reviews include Bahcall (1986), Gilmore & Wyse (1987), Freeman (1987), and Buser (1988).

2.1 *The Fundamentals of Star Count Analyses*

The number of stars N countable in a given solid angle to a given magnitude limit m is given by a simple linear integral equation, often known as "the fundamental equation of stellar statistics." It is

$$N(m) = \int \Psi(M_v, \mathbf{x}) D(M_v, \mathbf{x})\, d^3x, \qquad 5.$$

where $\Psi(M_v, \mathbf{x})$ is the distribution function over absolute magnitude and position, $D(M_v, \mathbf{x})$ is the stellar space density distribution, and d^3x is a volume element. This (Fredholm) equation is rarely invertable, since it is ill conditioned. A detailed discussion of its use and approximate solution upon inversion is presented by Trumpler & Weaver (1953, Chap. 5.5). In general, the luminosity function is too broad to allow any solution for *both* $D(M_v, \mathbf{x})$ and $\Psi(M_v, \mathbf{x})$. The situation can be improved by restricting the data by color and/or spectral type, which is the technique usually followed. In this case, for an assumed form of the distribution function $\Psi(M_v, \mathbf{x})$, the density function $D(M_v, \mathbf{x})$ is recovered from $N(m, \text{color})$. This may be done by inverting the data (classical photometric parallax) or computer calculation of the integral with subsequent iterative comparison of data and model (cf. Bahcall 1986). These techniques are clearly entirely equivalent and should agree. They often do not.

The fundamental problem with use of the fundamental equation is that both the stellar luminosity function and the stellar density law are functions of many parameters. Few of these are sufficiently well known to be fixed. Consequently, a wide variety of combinations of Ψ and D are allowed mathematically. Other *astrophysical* constraints are necessary, whose choice has remained subjective until recently owing to the lack of adequate observational constraints.

2.2 *The Choice of Astrophysical Constraints*

The technique adopted by almost all workers to date is to fix the very large number of parameters by adopting empirically determined fitting functions for quantities such as the density laws and luminosity functions, and then fitting a set of these fitting functions to the observations [the exception being the analysis of Robin & Crézé (1986a,b), who derive all relevant relations from a model of Galactic evolution]. The empirical fitting functions are determined primarily from photometric observations of spiral

galaxies thought to be similar to the Milky Way, from the Gliese catalogue of nearby stars, and from a small number of well-studied globular and open clusters. As most authors are forced to adopt the same few fitting functions, in the absence of any alternatives, it is not surprising that most conclusions are similar. Analyses of this type were pioneered by van den Bergh (1979). Later models have been published by Bahcall & Soneira (1980, 1981, 1984), Bahcall et al. (1985), Gilmore (1981, 1983, 1984b), Gilmore & Reid (1983), Gilmore et al. (1985), Brooks (1981), Yoshii (1982), Pritchet (1983), Buser & Kaeser (1985), Robin & Crézé (1986a,b), Friel & Cudworth (1986), Yoshii et al. (1987), Hartwick (1987), del Rio & Fenkart (1987), Sandage (1987a,b), and Fenkart (1989 et seq), and Rodgers & Harding (1989).

Some of the adopted constraints have recently been discovered to have been poorly justified. The most important example of this is the popular impression that the photometric properties of spiral galaxies are adequately described as a sum of a flat exponential (both radially and vertically) disk and a roughly round spheroid described by the $r^{1/4}$ law when seen in projection. Recent photometric analyses have shown that such a description is an unacceptably poor description of high-quality surface photometric data in almost all cases (Schombert & Bothun 1987, Shaw & Gilmore 1989). Rather, the luminosity profile of NGC 891, the galaxy often quoted to be most like the Milky Way, shows no evidence for a detectable $r^{1/4}$ component in its luminosity distribution (Shaw & Gilmore 1989). Thus, one should not necessarily expect a star count model based on an $r^{1/4}$ spheroid to be an adequate description of the Milky Way.

A specific point of interest in the recent star count literature has involved the parameters of the thick disk, with some conflicting claims as to its reality until a few years ago, when the evidence from several kinematic and spectroscopic surveys became overwhelming (cf. for example, Sandage & Fouts 1987, Sandage 1987a,b, Carney et al. 1989a). This apparent uncertainty in the star count modeling was due to the extreme sensitivity of computer models to the adopted stellar luminosity function and color-magnitude relations. Unless careful astrophysical constraints are imposed on these choices, a huge variety of models is possible that can reproduce the data. This is well illustrated by the "disproof" of the existence of a thick disk by Bahcall & Soneira (1984, Figure 19). They showed the complete disagreement of such a model with the faint stellar data of Kron in SA 57. In a later paper, however, Bahcall et al. (1985, Figure 19) showed the excellent fit of the same geometric model to the same data. The only difference in the latter case was the use of a luminosity function that is appropriate for an old stellar population, as required by the color data, expected for a spheroidal population, and earlier derived by Gilmore & Reid (1983).

The uncertainties above illustrate the fundamental limitation of the modeling of star count data in isolation, which is a severe restriction on its value—too few constraints are usually available to provide a unique model, and too few consistency arguments are usually applied during its use. One requires additional information other than star count data to constrain the appropriate color-magnitude relation and, if possible, kinematic data to allow segregation of different stellar populations. The color-magnitude relation of a stellar population is a function of chemical abundance and age, while the density law depends on both the stellar kinematics and the gravitational potential gradients. In general, none of these parameters is known adequately a priori.

Essential supplementary information is available from kinematics (particularly proper-motion and radial velocity surveys) and from spectroscopic surveys. The latter allow dwarf-giant discrimination, provide chemical abundance data, and hence allow the derivation of reliable distances. Both kinematic and spectroscopic data have become available in large quantities in the last few years, and are being included in star count modeling. Proper-motion data for bright stars ($V < 6$) have been included in a two-component disk/spheroid model by Ratnatunga et al. (1989). As a result of the restriction to bright, and hence nearby, stars, the results of such modeling are highly specific to the kinematic properties of young stars near the plane of the Milky Way—plausible mean values from the literature for the local kinematics were able to fit the data in their modeling only to within 25%. Extension of analyses of this type to the high-precision, high-statistical weight HIPPARCOS catalogue and to the Lick proper-motion survey (Klemola et al. 1987) will be of considerable interest. The results of the several spectroscopic surveys, which have provided conclusive evidence for the existence of a Galactic thick disk with descriptive parameters similar to those proposed by Gilmore & Reid (1983), are discussed in Section 4 below.

2.3 *Analysis of Star Count Data*

The most straightforward analysis technique for stellar number–magnitude–color data is photometric parallax. This involves use of the absolute magnitude–color relation for a galactic or globular cluster of appropriate chemical abundance. The absolute magnitude for a field star of measured color is read directly from this diagram and combined with the apparent magnitude to give a photometric distance. From a large set of distances, with appropriate Malmquist corrections, a density law can be derived directly. This technique has been extensively applied by the Basel group (R. P. Fenkart et al.) and by Gilmore & Reid (1983). The steep density profile from 2 kpc to 4 kpc was identified by these latter authors as a

Galactic thick disk, with exponential scale height ~ 1.3 kpc and local normalization $\sim 2\%$ of the old disk stars. They emphasized that a flattened $r^{1/4}$ law was an equally good fit to the data. A density profile of steep exponential form at distances of a few kiloparsecs from the Galactic plane was in fact very well established many years ago [cf. reviews by Elvius (1965, especially Figure 2) and Plaut (1965, especially Figure 7b)] though evidently forgotten. Similar results to those of Gilmore & Reid were earlier derived from the Basel surveys by Yoshii (1982), though not widely appreciated at that time. Yoshii showed that the Basel north Galactic pole star count data required the vertical density profile of the dominant stellar population more than ~ 1.5 kpc from the Galactic plane to follow an exponential density distribution with scale height a factor of ~ 6 larger than that of the old disk. The corresponding factor derived by Gilmore & Reid from their exponential fits to the south Galactic pole data was ~ 4. More recently Yoshii et al. (1987) have analyzed new data for the north Galactic pole and derived a scale height ratio of thick disk : old disk of ~ 3, again similar (though not identical) parameters to those of Gilmore & Reid.

The alternative analysis technique involves the direct calculation of the integral in the fundamental equation of stellar statistics. This is a straightforward computational exercise. Consequently, many attempts have been made recently to explore parameter space so that the uniqueness of the results from the direct analysis of star count data can be determined. In relevant form, this equation is

$$N(V, B-V) = w \int \Psi\left(M_v, \left[\frac{A}{\mathrm{H}}\right], \tau, r, \ldots\right) D(r, M_v, \tau) r^2 \, dr, \qquad 6.$$

where τ is stellar age, $[A/\mathrm{H}]$ is stellar elemental abundance, and w is observed solid angle. The luminosity function Ψ (stars mag^{-1} pc^{-3}) has been known for many years to be a function of distance from the Galactic plane (e.g. Bok & MacRae 1942). Similarly, the existence of age-velocity dispersion and age-metallicity relations for old thin disk stars is well known. This emphasizes the crucial and irreducible limitation of analyses of this type—both the luminosity function and the density law are functions of the other phase-space parameters. A unique solution of Equation 6 is therefore impossible. Instead, a large number of parameters must be fixed on external astrophysical grounds. Additionally, comparison with observational data requires adoption of an appropriate absolute magnitude–color relation, in exactly the way required in the more direct photometric parallax analysis technique described above. It is this nonuniqueness that must be overcome by the use of supplementary chemical abundance

and stellar kinematic data. We emphasize that star count analyses *in isolation* are incapable of providing a unique description of the structure of the Galaxy. The results of any such analysis should be viewed as merely indicative of the type of combination of fitting functions that can be used to represent available data. They should not be accepted as a valid description of the stellar populations in the Galaxy until the chemical abundance, luminosity class, age, and kinematic assumptions are tested by spectroscopic observations.

2.4 *Available Modern Star Count Data*

The availability of high-efficiency, linear, two-dimensional detectors (CCDs) and fast, automated, photographic plate-scanning microdensitometers (PDS, COSMOS, APM) has revolutionized stellar statistics. Complete samples of stars can be measured to useful precision in several wavebands over sufficiently large areas of sky that random errors due to counting statistics are unimportant. The minimization of systematic errors still requires an enormous effort, however [cf. Gilmore (1984a) for a description of the requisite photometric techniques]. Table 1 of Gilmore & Wyse (1987) summarizes those recent high-Galactic-latitude studies in which the magnitude calibration was derived directly from photoelectric or CCD standards. With the conspicuous exception of work by the Basel group (R. P. Fenkart et al.; see below), no substantial new data sets have been published since that table was prepared.

The general features of the high-latitude sky are illustrated in Figure 2, which shows stellar photometric data derived from APM scans of high-

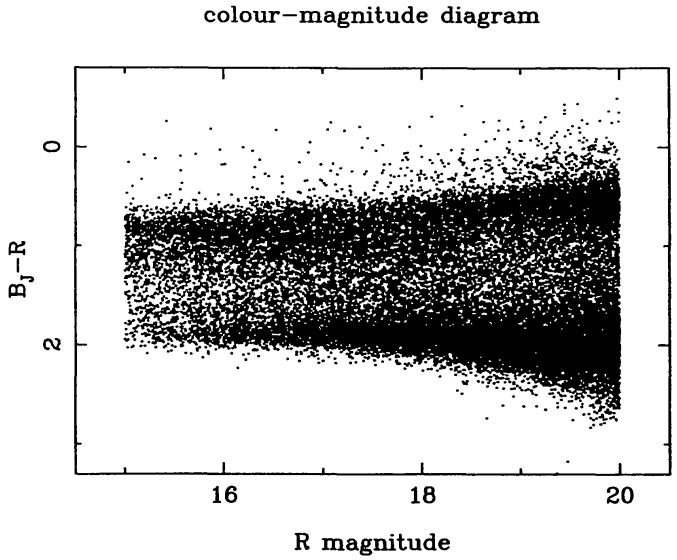

Figure 2 A representative color-magnitude diagram of the stellar distribution in the high-latitude sky. This is derived from APM scans of UK Schmidt Telescope plates.

Galactic-latitude plates from the UK Schmidt Telescope. The important aspects of these data are the following:

1. The sharp edge to the distribution near the equivalent of $B-V = 0.4$, with very few stars being seen significantly bluer than this limit. This corresponds to the main-sequence turnoff color of an old, metal-poor population. The absence of a younger turnoff shows that no substantial continuing star formation has taken place in the spheroid—though note the existence of some apparently young high-latitude metal-rich A stars, whose place of formation remains an extremely important mystery (Lance 1988), and some distant B stars that cannot have traveled from the thin disk in their main-sequence lifetimes (Keenan et al. 1986, Conlon et al. 1988).
2. The peak of the distribution near the equivalent of $B-V = 0.6$. This is similar to the main-sequence turnoff color of metal-rich globular clusters and shows the mean abundance of the field spheroid sampled here to be approximately -0.5 to -1 dex. The consequences of this for the age of these stars are discussed in Section 3.
3. The peak of the distribution near the equivalent of $B-V = 1.5$. This feature corresponds to the insensitivity of blue colors to effective temperature in cool main-sequence stars. It is therefore an artifact of the choice of photometric pass-bands rather than evidence of a structural property of the Galaxy. This is best illustrated by comparison with Figure 3*b* of Gilmore & Wyse (1987), which shows $V/V-I$ data for the same stars as are shown in Figure 2. The continuing temperature sensitivity of the $V-I$ color leads to the very different appearances of the two diagrams.
4. The absence of a large number of stars at the red edge of the distribution at faint apparent magnitudes. Such very red stars are very cool low-mass M dwarfs and have often been hypothesized as candidates for the local missing mass. Their absence in this diagram was the first direct evidence that low-mass luminous stars do not contribute significantly to the mass density in either the disk (Gilmore & Reid 1983) or the halo (Gilmore & Hewett 1983) of the Galaxy. [We also note that the observations and analyses that suggested the need for missing mass associated with the disk of the Galaxy have been superseded (see Section 5 below) by new data and analyses that suggest that there is no missing mass associated with the Galactic disk.]

The appearance of Figure 2 does not change significantly to $V \sim 22$ (Kron 1980). At fainter magnitudes it is expected that the blue edge will move to progressively redder colors as intrinsically fainter subdwarfs dominate the counts.

The most useful external estimates of the accuracy of the data come from observations of the Galactic poles, as only there do truly independent duplicating data exist. For the south Galactic pole, observations exist by Bok & Basinski (1962), Reid & Gilmore (1982), and Gilmore et al. (1985) in the Johnson *BV* system. For the north Galactic pole, similar data have been published by Weistrop (1972), Chiu (1980), and Stobie & Ishida (1987). The detailed counts from these sources are compared in Figures 5 and 6 of Stobie & Ishida (1987), showing that the various authors agree to within $\sim 5\%$ for apparent magnitudes brighter than about $V = 18$.

At apparent magnitudes fainter than $V = 18$ and in other directions, only one other such comparison is possible, and this is detailed in Gilmore et al. (1985). Similar precision is suggested to $V \lesssim 21$. At fainter magnitudes the precision of the star count data becomes dominated by the difficulties of reliable star-galaxy separation, leading to *systematic* errors whose amplitude is impossible to quantify from extant data (cf. Section 2.6). The best available estimate of the external accuracy of modern automated photographic data that is directly calibrated by a large number of photoelectric and/or CCD standards is about 10% in both apparent magnitude and color for $V \lesssim 21$. The internal precision is typically a factor of two better.

2.5 *Star Counts and Stellar Components*

Interpretation of the parameters of star count models—specifically the relative fractions of stars near the Sun assigned to discrete density distributions and characterized by a specific color-magnitude relation—in terms of stellar populations is an ambitious task. In principle, it is possible so long as supplementary chemical abundance, age, and kinematic data are available. (These supplementary data are discussed in Section 4 below.) Nevertheless, it is a worthwhile exercise to test the validity of the geometrical aspects of current star count models by comparing them with observations in directions other than those from which the model parameters have been derived.

2.5.1 STAR COUNTS AND THE THICK DISK By far the most extensive star count data set available is that obtained for the Basel Halo Program. This very large program has been in operation for 25 years, has provided three-color data in 15 separate fields, and is currently being summarized and analyzed in a series of four papers by R. Fenkart (1989 et seq; see also Buser 1988). Fenkart has emphasized the very good agreement between the thick disk density law derived by Gilmore & Wyse (1985), including an exponential profile for the thick disk and a color-magnitude relation like that of a metal-rich globular cluster, and that required by the Basel

data in many fields at both high and low Galactic latitudes. This provides the first evidence for the global applicability of the thick disk parameters derived by Gilmore & Reid and by Gilmore & Wyse. Independent confirmatory evidence is provided by McNeil (1986), who derived the density profile of spectroscopically selected M giants toward the south Galactic pole and derived a density profile similar to that discussed above. [This sample has some overlap with the Hartkopf & Yoss (1982) sample of K giants, the kinematics of which is discussed in Section 4 below.]

When comparing observations with the predictions of the several star count models, however, it is essential to bear in mind the limitations of the available models. While the thick disk model is in good agreement with a wealth of star count, chemical abundance, spectroscopic luminosity-classification, and radial velocity data [see Freeman (1987) and Section 4 below], almost all high-precision data are restricted to the range from a few hundred to a few thousand parsecs from the Sun. The original set of parameters describing the thick disk were derived solely to reproduce the observed stellar distribution from $\sim$1 kpc to $\sim$4 kpc from the Galactic plane toward the south Galactic pole. While parameters similar to those originally derived have subsequently been found to provide a good description of the data in several other high-latitude fields [e.g. Yoshii et al. (1987) for the north Galactic pole; Fenkart (1989) et seq], extrapolation of the fitted exponential well outside the range over which it has been verified is certainly not guaranteed to be an adequate description of the Galaxy.

Determinations of the local thick disk normalization by extrapolation of the thick density law derived from star counts down to the Galactic plane—i.e. by extrapolation of the density from $z \sim 1$ kpc to $z \sim 0$ kpc—yield values from $\lesssim$1% to a few percent of the local total stellar density, although Sandage (1987b) quotes 10%, with a lower value of the scale height than the other determinations. The *physical* local normalization can be determined from the distant data only if one knows the vertical Galactic force law as a function of z-distance from the plane, $K_z(z)$, and the velocity distribution function over the range of interest (Sandage 1987b). It is quite unrealistic that an extrapolated exponential will be a valid description of the space density of thick disk stars near the Sun, which complicates attempts to identify specific local candidate stars. The physical significance of the local normalization is further discussed by Evans (1987). The most recent determination of the vertical density profile of the Galaxy is derived from a sample of K dwarfs, with luminosity classification and abundance corrections to the absolute magnitude derived from high quality spectra, analyzed by Kuijken & Gilmore (1989b; cf. Section 5). Their density distribution is well described by the double-exponential fit

$$\frac{\nu_0(z)}{\nu_0(0)} = 0.959e^{-z/249\,\mathrm{pc}} + 0.041e^{-z/1000\,\mathrm{pc}}. \qquad 7.$$

This fit was made to the star count data over the z range 300–4000 pc, where the lower limit was chosen to avoid any residual giant contaminations of the sample. The individual exponential scale heights quoted are not to be interpreted as definitive. The numerical values are very highly anti-correlated, and other equally acceptable double-exponential fits exist. A density profile that does not include a few percent of the stars near the Sun in a component of the Galaxy with a characteristic scale height of ~ 1 kpc is, however, quite inconsistent with observations.

2.5.2 STAR COUNTS AND THE CENTRAL BULGE One situation in which the current star count models appear not to provide an adequate description of the Galaxy is in lines of sight within $\sim 30°$ of the Galactic center. In these directions, available data (Rodgers et al. 1986, Rodgers & Harding 1989, Gilmore & Hewett 1989) show a substantial *excess* of stars above the predictions of the models. The available data are somewhat confusing, however, and are not consistent with a simple extra "bulge" population superimposed on the basic disk–thick disk–spheroid model of the Galaxy. It does seem that there is a contribution to the stellar distribution in the central regions of the Galaxy that has a scale length of ~ 1 kpc. (For comparison, the classical subdwarf system has a half-light scale length of ~ 3 kpc.) This population also seems to have a rather blue (F star) main sequence turnoff, suggestive of a young age and/or a low chemical abundance. The available photometry is, however, inadequate to produce definitive parameters, owing to the complexities of photometry in crowded fields, the effects of patchy reddening, and the need to survey many fields to describe the apparent distribution of stars adequately. Spectroscopic and photometric studies to clarify this uncertainty are underway.

One of the most important implications of data within a few kiloparsecs of the Galactic center is that one expects to see a flaring of the old disk and the thick disk in these regions. Lewis & Freeman (1989; see also Freeman 1987) have shown that the planar, radial velocity dispersion of the old disk rises exponentially toward the Galactic center, with a scale length twice that of the luminosity. This is the predicted behavior for a constant scale height, radially exponential disk, assuming that the ratio of the vertical to the radial velocity dispersions remains roughly constant (see Section 3.1 and van der Kruit & Freeman 1986). Thus there will exist a radius within which the old stars of the "disk" become of sufficiently high velocity dispersion—both radial and vertical—that their spatial configuration will no longer be specified predominantly by angular momentum

support, but will also be determined by a significant contribution from pressure support. The stellar system will puff up, and the higher velocity dispersion thick disk will transform itself into a "bulge" population. This model (i.e. that the "bulge" is the inner regions of the thick disk) has a conspicuous advantage over explanations of the central bulge as being part of the inward extension of the local subdwarf system in that it naturally accounts for both the high chemical abundance and the high stellar rotation velocities observed in external galactic bulges. This point is discussed further by Jones & Wyse (1983), King (1986), and Wyse & Gilmore (1988).

The relation of the stars seen from $\sim$15–30° from the Galactic center to the highly concentrated (within $\lesssim$1 kpc of the Galactic center) stellar distribution remains unclear. Frogel (1988) reviews the evidence concerning the age of the majority of stars in the central bulge and concludes that they are old, similar to the thick disk globular clusters (see also Terndrup 1988). However, there are contradictory indications. The late-type stars seen by the *IRAS* satellite (Habing 1987, Harmon & Gilmore 1988) are long-period variables with young ages, and both the *IRAS* sources and the late-spectral-type M giants form a stellar system with scale length an order of magnitude smaller than that of the subdwarf system (Blanco & Blanco 1986). The very uncertain direct age determinations for the K giants in Baade's Window (Terndrup 1988) allow a substantial age gap, of order 7 Gyr, between these stars and the oldest subdwarfs. Thus the relation of the dominant stellar population within the central few kiloparsecs of the Galaxy to the dominant population several kiloparsecs from the center and from the plane remains problematic (see also Section 1.3). The former, however, is metal rich, may be of intermediate age, and forms a high-velocity-dispersion yet predominantly rotationally supported system; the latter is metal poor, apparently exclusively old, and forms an entirely pressure-supported system. The assumption that the former is the inward extension of the latter is far from trivially consistent with observations.

2.6 *The Shape of the Metal-Poor Spheroid*

As an example of the type of analysis for which star counts are ideal, we discuss a recent determination (Wyse & Gilmore 1989) of the shape of the metal-poor spheroid, represented in the solar neighborhood by the high-velocity subdwarfs. The shape of the non–thin disk stars is important because of its implications for the early stages of galaxy collapse and star formation, the interpretation of the kinematics of high-velocity stars, and the shape of the underlying dark matter that generates the gravitational potential in which these stars move.

As discussed further in Section 3.1, the high-velocity, metal-poor field

stars in the solar neighborhood have an anisotropic velocity dispersion tensor, with $\sigma_{rr}:\sigma_{\theta\theta}:\sigma_{zz} \sim 2:1:1$ derived from kinematically unbiased samples. Since the velocity dispersion tensor behaves as an anisotropic stress tensor in the equations governing stellar dynamics, one may expect this anisotropic "pressure" to result in an anisotropic shape, i.e. a flattened metal-poor spheroid (see Section 3.1 for the relevant equations). Binney & May (1986) investigated this idea in more detail for various Galactic potential–distribution function pairs and concluded that in the locally nonspherical potential felt by the subdwarfs, owing to the presence of the disk, the observed velocity dispersion anisotropy implies a substantially flattened spheroid, with shape $\sim$ E7 or axis ratio ~ 0.25. A spherical potential would imply shape $\sim$ E3, with axis ratio $c/a \sim 0.7$. White (1989b) quantified the expectation of a flattened shape resulting from a flattened velocity ellipsoid using the tensor virial theorem for axisymmetric galaxies. This approach has the disadvantage of treating the two components of the velocity dispersions tangential to the vertical direction on an equal footing, which is not compatible with the observations, but the general results should be valid. Adjusting his results to reflect the *nonkinematically selected* velocity dispersions, one finds from the flattening of the velocity ellipsoid that in a spherical potential the subdwarfs should have axis ratio $c/a \sim 0.4$, while in a potential due to a mass distribution that is also flattened one obtains $c/a \sim 0.3$. The ratio of the vertical velocity dispersion to the circular velocity also constrains the flattening and predicts $c/a \sim 0.53$. The precise numerical value for this flattening is model dependent and hence uncertain, though the general conclusion that the subdwarf system must be appreciably flattened is robust.

The kinematic data of Ratnatunga & Freeman (1985, 1989) for distant metal-poor K giants can also most easily be explained by allowing these stars to form a flattened distribution. The most important feature of their data is the fact that the line-of-sight velocity dispersion in the south Galactic pole may not increase with distance, despite the increasing contribution of the radial (relative to the Galactic center) component of the velocity dispersion (σ_{rr}) to the observed line-of-sight stellar radial (relative to the Sun) speed. The assumption behind the expectation of a rising line-of-sight dispersion with distance is that the distant metal-poor K giants trace the same population as the local metal-poor K giants and the local subdwarfs, and hence they should have the same radially biased velocity-dispersion tensor. Adopting a global form of the distribution function in either a spherical (White 1985) or in an oblate (Levison & Richstone 1986) potential requires a flattened spatial distribution for the spheroid stars, again with axis ratio ~ 0.25. Alternatively, one can depress the observed velocity dispersion at large distances by allowing suitable discontinuities

in the stellar distribution function—that is, by essentially assuming that all stars beyond a given Galactocentric radius are on circular orbits. This latter approach allows a fit that is consistent with a spherical spatial distribution for these stars, though at the expense of a somewhat contrived distribution function (Sommer-Larsen 1987, Dejonghe & de Zeeuw 1988, Sommer-Larsen & Christensen 1989), which as shown by White (1989b) cannot be globally applicable.

In the light of this kinematic evidence and the results of the more straightforward dynamical analyses, it is mildly puzzling that direct star count studies suggest that the subdwarf stellar system is approximately round [cf. Freeman (1987) for a review]. The most quoted evidence for a spherical distribution of field spheroid stars comes from the modeling by Bahcall & Soneira (1980, 1981, 1984; hereafter BS) of the faint star counts of Koo & Kron (1982) in two fields; BS conclude that the axis ratio of the spheroid stars is $c/a = 0.80^{+0.20}_{-0.05}$. Their technique is based on the fact that fields in the $l = 90°,270°$ plane are at equal Galactocentric distances if at equal distances from the solar neighborhood, and hence a spherical distribution of stars will contribute equally to all fields in this plane. Thus, if one compares magnitude-limited samples in fields at high and low Galactic latitude, one should obtain equal numbers of spheroid stars in the two fields. A flattened distribution of stars will yield lower counts in the higher latitude field.

BS complicate their analysis somewhat by adopting different color magnitude relations for the two fields, and thus they do not predict equal numbers of stars for a spherical distribution—they are forced to do this to obtain an acceptable fit for their model in each of the two fields, owing to a combination of inadequacies in the model (such as lack of the thick disk component) and in the data (discussed below). There is no physical basis for such a variation of color-magnitude relations (metallicity gradients are not relevant, since the fields are supposed to be at the same Galactocentric distance), and it is a potential source of uncertainty. Adoption of a metal-poor color-magnitude relation has the effect of assigning a low intrinsic luminosity to main-sequence stars of a given color. Hence, in an apparent-magnitude-limited sample, one will be comparing lower luminosity, less distant stars in the "metal-poor" field with higher luminosity, more distant stars in the other field. The predictions of relative star counts are therefore sensitive to the shape of the subdwarf luminosity function, as well as to the shape and density profile of the stellar tracer population. It is then possible to produce predictions for the ratio of counts that can exceed unity in a spherical distribution, as BS derived.

A new study of this problem, utilizing a larger data set and using a more general model Galaxy program that requires internally consistent

properties for a given stellar population in different fields, and that allows the inclusion of a thick disk, is described by Wyse & Gilmore (1989). Following BS, they counted stars blueward of a color limit ($B-V=0.6$) chosen to minimize contamination of the tracer sample by nearby old disk stars, with the precise value of this limit not being critical. The two fields used were ($l=0°$, $b=90°$; area surveyed = 0.75 square degrees) and ($l=272°$, $b=-44°$; area surveyed = 0.75 square degrees). The observed ratio of blue stars in the two fields was 0.59. This disagrees strongly with Koo & Kron's (1982) counts in two fields at similar Galactic latitudes but at much fainter magnitudes, which yield a ratio of 1.09 for blue stars with $20 \lesssim V \lesssim 22$; the more recent calibration of the Koo & Kron data by Koo et al. (1986) gives 1.3. (Note that these numbers are based on a somewhat uncertain color cut, but this should not matter provided one is blue enough to have isolated the metal-poor spheroid stars.) We suspect that this apparent disagreement reflects the uncertainty in the Koo & Kron counts due to the difficulty of reliable star-galaxy discrimination at faint magnitudes. This suspicion is based on the results shown in Table 1, which shows the Koo et al. (1986) "subdwarf" category counts for their north Galactic pole field, together with predictions from the Gilmore & Wyse (1985; henceforth GW) model and from the BS model, each model with an assumed spheroid axis ratio of 0.8. There is an obvious disagreement between the data and the models; the data fail to increase toward fainter magnitudes, contrary to both of the models and to intuition.

The BS model predictions (their Table 3) combined with the low value of the relative observed counts would imply that the spheroid had an axis ratio $c/a \lesssim 0.5$. When one considers the presence of the thick disk and also models the observed *total* counts as well as their ratio, the best estimate for the axis ratio of the metal-poor subdwarf stellar population within a few kiloparsecs of the Sun is $c/a \sim 0.6$. Note that this is 4σ below the quoted errors of BS, which illustrates the importance of systematic errors in these analyses.

One can also utilize direct counts of other spheroid tracers, such as RR Lyrae stars, to derive the density profile of spheroid light. Early work based on RR Lyrae stars in the Palomar-Groningen and Lick surveys, which were toward the Galactic center (Kinman et al. 1966, Oort & Plaut 1975), concluded that these stars were distributed in a nearly spherical system. These results have now been superseded by better photometric data (Wesselink et al. 1987); the more modern analysis finds, in contrast, that the RR Lyrae stars toward the Galactic center have a rather flattened distribution, with axis ratio $\lesssim 0.6$, in excellent agreement with the star count result above. A possible complication in this picture was introduced by the results of a kinematic analysis by Strugnell et al. (1986), who showed

Table 1 Star count constraints on the slope of the Galaxy

Koo et al. (1986) north Galactic pole data; relative star counts

J mag	Data	V mag	BS model	GW model
20.25	1.0	19.75	1.0	1.0
20.75	0.8	20.25	1.1	1.2
21.25	1.0	20.75	1.24	1.39
21.75	1.1	21.25	1.35	1.57
22.25	1.0	21.75	1.45	1.73
22.75	0.8	22.25	1.57	1.91

Constraints on the spheroid axis ratio

Model	$(l, b) = (0, -90)$		$(l, b) = (270, -45)$		Relative counts	
Axis ratio	Thick disk	Spheroid	Thick disk	Spheroid	Spheroid	Total
1.0	20	367	60	368	1.00	0.90
0.75	20	215	60	279	0.77	0.69
0.6	20	133	60	209	0.64	0.57
0.5	20	86	60	156	0.55	0.49

Observed number counts

$(l, b) = (0, -90)$	$(l, b) = (270, -45)$	Ratio
168	284	0.59

that the c-type (low amplitude of variability) and the small ΔS (metal-rich) RR Lyrae stars have significantly different kinematics from the more metal-poor RR Lyrae stars. Thus the RR Lyrae stars, like other field stars, may well form a two-component system, with the more metal-rich stars being part of the thick disk. The need for more data on these stars is clear (see Sections 3 and 4 below).

Yet another complication in this picture is due to the analysis of Hartwick (1987), who analyzed the available data for *metal-poor* RR Lyrae stars and concluded that the axis ratio of the metal-poor RR Lyrae system varies with Galactocentric radius, being flattened [axis ratio $c/a \sim 0.6$ and scale height ~ 1.5 kpc (i.e. rather similar to the parameters of the more metal-rich thick disk RR Lyrae stars)] interior to the solar circle. At very large Galactocentric distances the RR Lyrae data somewhat favor a more spherical distribution. Hartwick thus suggested that the *metal-poor* RR Lyrae stellar system is itself two component, in addition to the (third)

metal-rich RR Lyrae system. As we discuss further below (Section 4.3), there are indications of a "metal-poor thick disk" in other samples of field stars.

Hartwick also finds a similar two-component structure for the metal-poor ([Fe/H] < -1) globular clusters from the distribution of their projected positions on the sky. Again, this two-component structure is additional to the well-established distinction between metal-rich and metal-poor clusters (Zinn 1985, Thomas 1989), where the metal-rich clusters form a clear disklike system. However, the small number of clusters involved gives Hartwick's multicomponent model small statistical weight. The kinematics of the metal-poor globular cluster system was found by Frenk & White (1980) to be describable by negligible net rotation and an isotropic velocity dispersion tensor. These properties suggest a spherical spatial distribution in a spherical potential and a flattened distribution in a flattened potential. However, Norris (1986) found there to be no statistically significant difference between the "isotropic" velocity dispersion tensor of the globular clusters and the markedly *anisotropic* velocity dispersions of the local subdwarfs, while Thomas (1989) has shown that one cannot in general draw *any* strong conclusions about the kinematics of the metal-poor globular cluster system, owing to the effects of distance errors.

Even if there were reliable evidence for a similarity between the kinematic parameters describing one or the other of the globular cluster systems and those describing the spheroid or thick disk field stars, this would not prove that the globular cluster and field star systems have a similar or common origin. Other parameters do appear to differ significantly. The most recent comparisons of the metallicity distributions of the globular clusters and the metal-poor field spheroid stars show statistically significant differences (Laird et al. 1988b), while Bell (1988a,b) and Schuster & Nissen (1989) provide suggestive evidence that the oldest field subdwarfs are older than the globular clusters. However, the latter conclusion rests on the uncertain need for an oxygen overenhancement in the stellar evolutionary calculations for globular cluster stars. The observational data regarding oxygen abundances in globular clusters are well reviewed by Kraft (1988), who shows the measured oxygen abundance to be quite different from star to star in a single cluster, with no clear conclusion regarding the appropriate abundance to be used for isochrone dating yet available. One should use considerable caution in deducing some property of the globular cluster systems from observations of the field star systems in the Galaxy, and vice versa.

In summary, the available evidence on the shape of the system of metal-poor field stars that make up the Galactic extreme Population II suggests that these stars form a distinctly nonspherical system, whose flattening

may vary with radius but is $c/a \sim 0.5$ within a few kiloparsecs of the Sun, and within a few kiloparsecs of the Galactic center.

3. KINEMATICS AND CHEMISTRY OF OLD STARS

The kinematic properties of stars in the Galaxy are related, through the gravitational potential Φ, to their spatial distribution. The scale length of the spatial distribution is determined by the total energy (kinetic and potential) of the stellar orbits, as well as by the gradient of the potential (i.e. the force on the star). The shape of the spatial distribution depends on the relative populations of the orbits supported by the potential and on the relative amounts of angular momentum (rotational) and pressure (stellar velocity anisotropy) balance to the potential gradients. The total orbital energy and angular momentum of a star depend on the maximum distance from the center of the Galaxy that the gas from which it will form reached before falling out of the background expansion of the Universe, the angular momentum of the gas clouds' orbit at that time, the depth of the potential well through which it fell, the fraction of the total orbital energy that was lost (dissipated) before the gas formed into a star, and the subsequent dynamical evolution of the stellar orbit. That is, the present kinematic properties of old stars in the solar neighborhood are determined in part by initial conditions in the proto-Galaxy at the time of the first star formation and in part by physical processes during galaxy formation. Hence, local kinematic studies can help to determine both the detailed physics of galaxy formation and also some of the large-scale structural properties of the Galaxy.

Stellar chemical abundance is determined by the fraction of the available interstellar medium (ISM) at the time and place of the star's formation that had been processed through the nuclear-burning regions of massive stars. It provides a valuable chronometer for the early evolution of the Galaxy. The chemical abundance of the ISM at any time depends both on the local history of formation and evolution of stars sufficiently massive to have created new chemical elements and on the mixing of local gas with more distant material. This more distant gas may or may not itself be enriched, so that the time-dependence of the chemical abundance of newly forming stars depends on both the local and the global star formation rates, the rate of infall of primordial gas, and the efficacy of mixing in the ISM. Thus, while the chemical abundance of newly formed stars is a valuable timepiece, this chronometer need not be a smooth or even a single-valued function of chronological time.

Clearly, however, the distribution function of stellar kinematics, chemistry, and age contains a wealth of information on the distribution of

proto-Galactic gas, the dissipational and star formation history of that gas, the subsequent dynamical history of the resulting stars, and the Galactic gravitational potential.

3.1 *Observable Stellar Dynamics*

The dynamics of any collisionless system, such as a large number of stars, is governed by the Vlasov equation, which is more commonly referred to as the collisionless Boltzmann equation (CBE):

$$\frac{Df}{Dt} \equiv \frac{\partial f}{\partial t} + \frac{\partial \mathbf{x}}{\partial t} \cdot \frac{\partial f}{\partial \mathbf{x}} + \frac{\partial \mathbf{v}}{\partial t} \cdot \frac{\partial f}{\partial \mathbf{v}} = \frac{\partial f}{\partial t} + \mathbf{v} \cdot \frac{\partial f}{\partial \mathbf{x}} - \nabla \Phi \cdot \frac{\partial f}{\partial \mathbf{v}} = 0, \qquad 8.$$

where f is the phase space density at the point $(\mathbf{x}, \mathbf{v})$ in phase space [i.e. there are $f(\mathbf{x}, \mathbf{v})\, d\mathbf{x}\, d\mathbf{v}$ stars in a volume of size $d\mathbf{x}$ centered on spatial coordinate $\mathbf{x}$, and with velocity in the volume of size $d\mathbf{v}$ about velocity coordinate $\mathbf{v}$]. The collisionless nature of stellar interactions allows the substitution of the gradient of the smoothed gravitational potential Φ for the accelerations. Here f does not have to describe the entire Galaxy; one can concentrate on any subsample of stars and apply the CBE (Equation 8) to it. We refer to such subsamples as *tracer populations*, since one can use their kinematics to trace the gravitational potential of the Galaxy, irrespective of the nature of the mass distribution that generates this potential. For stellar populations whose mass *generates* the potential as well as traces it, it is necessary to consider joint solutions of both the Boltzmann equation and the Poisson equation. Such *self-consistent* solutions are discussed in Section 5 below, where the local thin disk is discussed.

Since this review is concerned mostly with the old stellar populations, and primarily with high-Galactic-latitude distributions, we may safely assume that we are concerned with a steady-state tracer population in an axisymmetric time-independent potential, so that time- and ϕ-derivatives are zero.

It is then convenient to write the collisionless Boltzmann equation in cylindrical polar coordinates (r, ϕ, z):

$$v_r \frac{\partial f}{\partial r} + v_z \frac{\partial f}{\partial z} + \left(K_r + \frac{v_\phi^2}{r} \right) \frac{\partial f}{\partial v_r} - \frac{v_r v_\phi}{r} \frac{\partial f}{\partial v_\phi} + K_z \frac{\partial f}{\partial v_z} = 0, \qquad 9.$$

where the accelerations $\dot{v}_r, \dot{v}_\phi, \dot{v}_z$ have been equated to the forces that cause them, ϕ-gradients in f and in the potential have been set to zero, and $K_r \equiv -\partial\Phi/\partial r$ and $K_z \equiv -\partial\Phi/\partial z$ are the components of the gravity force. Clearly, knowledge of $f(\mathbf{x}, \mathbf{v})$ allows the force components K_r and K_z to be derived. Note, though, that any general function f of two variables need not allow a solution for K_r and K_z. In view of the intractability of the

general problem of solving the CBE, one proceeds in general by taking velocity moments. Multiplying through by v_z and by v_r and integrating over all of velocity space produces the Jeans' equations:

$$vK_z = \frac{\partial}{\partial z}(v\sigma_{zz}) + \frac{1}{r}\frac{\partial}{\partial r}(rv\sigma_{rz}), \qquad 10.$$

$$vK_r = \frac{1}{r}\frac{\partial}{\partial r}(rv\sigma_{rr}) + \frac{\partial}{\partial z}(v\sigma_{rz}) - \frac{v\sigma_{\phi\phi}}{r} - \frac{v}{r}\langle v_\phi\rangle^2, \qquad 11.$$

where $v(r,z)$ is the space density of the stars, $\sigma_{ij}(r,z)$ their velocity dispersion tensor, and the only mean streaming motion is rotation, $\langle v_\phi\rangle$.

Each of the two force components can, in principle, be derived from the measurements of the moments of the velocity distribution and of the spatial density distribution of a tracer stellar population. Such experiments have been carried out for the z-force and relate the stellar kinematics and space density to the potential of the Galactic disk. They are discussed further in Section 5. It is convenient for present purposes to rewrite the radial equation (Equation 11) in terms of observables in the Galactic plane ($z = 0$). We obtain

$$v_c^2 - \langle v_\phi\rangle^2 = \sigma_{\phi\phi} - \sigma_{rr} - \frac{r}{v}\frac{\partial(v\sigma_{rr})}{\partial r} - r\frac{\partial\sigma_{rz}}{\partial z}$$

$$= \sigma_{rr}\left\{\frac{\sigma_{\phi\phi}}{\sigma_{rr}} - 1 - \frac{\partial \ln(v\sigma_{rr})}{\partial \ln r} - \frac{r}{\sigma_{rr}}\frac{\partial\sigma_{rz}}{\partial z}\right\}. \qquad 12.$$

In this relation v_c is the circular velocity (i.e. $v_c^2 = r(\partial\Phi/\partial r) = -rK_r$, where we adopt a locally flat rotation curve with $v_c = 220$ km s^{-1} for this article), and $\langle v_\phi\rangle$ is the mean rotation velocity of the relevant sample of tracer stars, which has velocity dispersions $(\sigma_{rr})^{1/2}$, $(\sigma_{\phi\phi})^{1/2}$, and $(\sigma_{rz})^{1/2}$, and radial spatial density distribution $v(r)$ (recall that r is the *planar* radial coordinate). The quantity $v_c - \langle v_\phi\rangle \equiv v_a$ is often called the *asymmetric drift* of a stellar population.

Equation 12 relates measurable local moments of the stellar distribution function to global properties of the Galaxy. In order to illustrate its application, we discuss each term briefly.

♣$\sigma_{\phi\phi}/\sigma_{rr}$: The velocity dispersions at $z = 0$ of old disk stars are probably best estimated from the nearby, spectroscopically selected K and M dwarfs with good parallax distances. These give $\sigma_{rr}:\sigma_{\phi\phi}:\sigma_{zz} = 39^2:23^2:20^2$ (Wielen 1974). For low-metallicity field stars ([Fe/H] ≤ -1) the weighted mean values from Carney & Latham (1986), Norris (1986), and Morrison et al. (1989) are $\sigma_{rr}:\sigma_{\phi\phi}:\sigma_{zz} = (131\pm7)^2:(102\pm8)^2:(89\pm5)^2$. (Note that

these values are derived from *nonkinematically selected* samples.) The first term in Equation 12 then becomes $\sigma_{\phi\phi}/\sigma_{rr} = 0.35$ for the old disk and $\sigma_{\phi\phi}/\sigma_{rr} = 0.61$ for the low-abundance field stars.

♣$\partial \ln (v\sigma_{rr})/\partial \ln r$: The thin exponential disks of spiral galaxies are apparently self-gravitating (see Section 5) and are observed to have a constant thickness with radius and to be approximately isothermal vertically (van der Kruit & Searle 1982). Thus, since the scale height of a self-gravitating disk varies as $h_z \propto \sigma_{zz}/\Sigma$, with $\Sigma \propto \exp(-r/h_r)$ being the disk surface mass density, one expects that the radial variation of the vertical velocity dispersion will be $\sigma_{zz} \propto \exp(-r/h_r)$. Assuming that the shape of the velocity ellipsoid is independent of position (or, more specifically, that $\sigma_{rr} \propto \sigma_{zz}$) leads to

$$\frac{\partial \ln (v\sigma_{rr})}{\partial \ln r} = 2 \times \frac{\partial \ln v}{\partial \ln r} = -2h_r^{-1}r. \qquad 13.$$

We had to assume a form for the velocity ellipsoid above to close the system of equations owing to the lack of an analogue of the equation of state. For simplicity, we restrict discussion of spheroidal distributions to an isothermal spheroid $\sigma_{rr} =$ constant, so that

$$\frac{\partial \ln (v\sigma_{rr})}{\partial \ln r} = \frac{\partial \ln v}{\partial \ln r}. \qquad 14.$$

♣$(r/\sigma_{rr})(\partial\sigma_{rz}/\partial z)$: The term involving σ_{rz} describes the orientation of the velocity ellipsoid and has no general analytic solution. The velocity ellipsoid will be oriented along the coordinate system (if there is one) in which the Hamilton-Jacoby equation, which provides the equations of motion, is separable, though unfortunately there is no reason for there to be a simple relationship between this (Stäckel) coordinate system and the coordinate system in which observations are naturally available. We therefore consider two representative cases only. If the potential is that of an infinite, constant-surface-density sheet, the velocity dispersion tensor will be diagonal in cylindrical-polar coordinates and always point at the Galactic minor axis, so that $\sigma_{rz} \equiv 0$. This is the assumption most commonly adopted. An alternative idealization is to assume that the potential is dominated by a sufficiently centrally concentrated or spherical mass distribution that the local velocity ellipsoid points at the Galactic center. This assumption was made by Oort (1965), who found that $\sigma_{rz} \sim (z/r)(\sigma_{rr} - \sigma_{zz})$ for $z \ll r$, from which it follows that

$$\frac{r}{\sigma_{rr}} \frac{\partial \sigma_{rz}}{\partial z} \approx 1 - \frac{\sigma_{zz}}{\sigma_{rr}}. \qquad 15a.$$

An exact derivation for a disk in which the velocity ellipsoid has constant shape in spherical polar coordinates, with axis ratio $\sigma_{rr} = \alpha^2 \sigma_{zz}$ at $z = 0$, when spherical and cylindrical coordinates coincide (Kuijken & Gilmore 1989a) provides

$$\sigma_{rz} = \left[\frac{rz(\alpha^2-1)}{\alpha^2 z^2 + r^2}\right]\sigma_{zz},$$

so that

$$\frac{r}{\sigma_{rr}}\frac{\partial \sigma_{rz}}{\partial z} \approx (\alpha^2-1)\frac{\sigma_{zz}}{\sigma_{rr}}. \qquad 15b.$$

For the velocity dispersions quoted above, both Equation 15a and Equation 15b provide the same answer for the old disk, namely

$$\frac{r}{\sigma_{rr}}\frac{\partial \sigma_{rz}}{\partial z} \simeq 0.75, \qquad 15c.$$

while for the spheroidal field stars the numerical value from Equation 15a is 0.53. This range in values for the σ_{rz} term is one indication of the uncertainty in present applications of this equation. A second indication is that numerical orbit integrations in potentials derived from recent studies of the Galactic K_z force law (cf. Section 5 and Kuijken & Gilmore 1989a) show that the velocity ellipsoid tends to point somewhat above the direction to the Galactic center, so that these correction terms will slightly overestimate the amplitude of the term involving σ_{rz}. Neglecting this term (as is often done) is, however, clearly unjustified.

For an exponential disk of radial scale length h_r and a sample of stars observed in the solar neighborhood, Equation 12 therefore becomes

$$v_c^2 - \langle v_\phi \rangle^2 = \sigma_{rr}\left(2\frac{d_*}{h_r} - 1.4\right), \qquad 16a.$$

where d_* is the distance of the Sun from the Galactic center ($\sim$7.8 kpc; Feast 1987). Alternatively, for a spheroid with a power-law density distribution with exponent γ, i.e. $\nu(r) \propto r^{-\gamma}$, we have

$$v_c^2 - \langle v_\phi \rangle^2 = \sigma_{rr}(\gamma - 0.9). \qquad 16b.$$

Thus a stellar tracer population that belongs to an exponential distribution with scale length $\sim$3.5 kpc (a plausible value for the Galactic old disk) will follow a similar asymmetric drift relation to that of a tracer population that is part of an isothermal distribution describing an r^{-4} spheroidal density distribution. Also, note that the largest allowed radial velocity

dispersion, corresponding to zero net rotation, for such a stellar system with the observed anisotropic velocity dispersions is $\sim 1.2v_c/\sqrt{4}$, or ~ 135 km s^{-1}. For a tracer population with any smaller radial velocity dispersion, Equation 12 describes the interplay between the pressure (velocity anisotropy) support and the angular momentum (rotation velocity) support to the spatial distribution. A higher velocity dispersion system than this has larger total energy and will form a more extended system. One might also assume it would have formed from less dissipated material, which is of course the clue to the *physical* significance of Equation 12 and the reason for this extensive discussion of it here.

3.1.1 THE ASYMMETRIC DRIFT The relevant observational data are shown in Figure 3, where the data points shown have been either collated or calculated from data available in the identified references. The data from the large surveys have been binned by metallicity. It is apparent that all data for tracer samples with a Galactic rotation velocity greater than about 50 km s^{-1} are consistent with a single density distribution, with the marginally significant exception of the metal-rich globular cluster system, whose radial velocity dispersion is rather low. This datum is, however, somewhat more uncertain than most of the other data shown owing to distance and reddening uncertainties. The range of uncertainty (see Figure 4*a*) shown covers the solutions found by Armandroff (1989); his favored solution, which has high rotation velocity, contains only nine clusters. The data of Norris & Ryan (1989a,b) have not been plotted, since although the data for their (kinematically selected) sample show the same trend as the Sandage & Fouts (1987) sample, they are offset in rotation velocity and obscure the important point of the figure. The origin of this systematic difference between the data of Sandage & Fouts and those of Norris & Ryan is not yet clear.

Observational selection effects can have a very substantial effect on the appearance of the diagram and have not been considered at all adequately. Obvious examples include explaining the apparent systematic difference in the deduced radial velocity dispersion between spectroscopically and kinematically selected samples (cf. Norris 1986), even for the highest velocity stars, which are far from the regions of phase space expected to be affected strongly by the selection criteria. In addition, proper-motion samples will not find metal-poor stars on circular orbits near the Sun if they exist (see Section 4) with the same low local normalization as the high-velocity subdwarfs. Local surveys will also miss stars on high-angular-momentum, high-energy orbits, since these will always lie beyond the solar circle.

The mean density law consistent with the majority of the data cor-

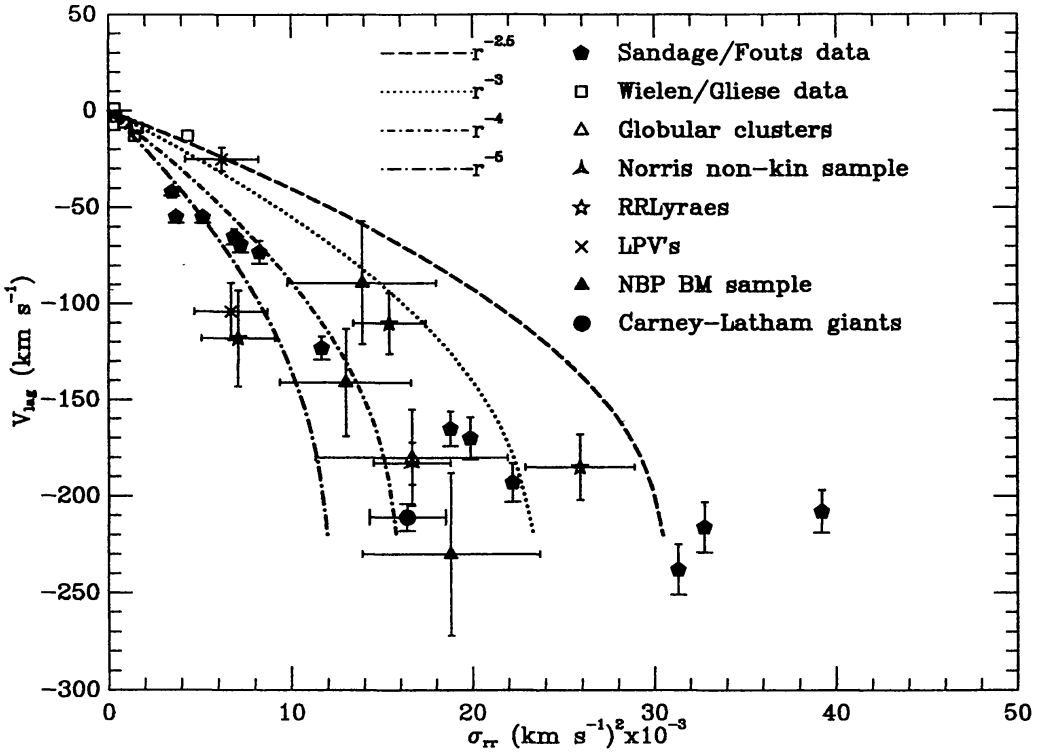

Figure 3 The relation between the radial velocity dispersion σ_{rr} and the asymmetric drift V_{rot} of samples of old stars in the Galaxy. The data for field stars are binned by metallicity. The key identifies data from the following sources: the proper-motion sample of Sandage & Fouts (1987) for stars with [Fe/H] $\gtrsim -2$ only, since photometric metallicities and hence distances are very uncertain for the more metal-poor stars; the Wielen (1974) analysis of the Gliese nearby star catalogue; the analyses by Norris (1986) of the globular cluster system and of kinematically unbiased low-abundance stars; the analysis by Strugnell et al. (1986) of field RR Lyrae stars; long-period variables (binned by period range) from the analysis by Osvalds & Risley (1961); spectroscopically selected low-abundance field stars from the analysis by Norris et al. (1985); and the spectroscopically selected local metal-poor giants from the study by Carney & Latham (1986). The model lines correspond to different solutions of Equation 12. The following density laws were used: $r^{-2.5}$ (long dashes), r^{-3} (dots), r^{-4} (short dash–dot), and r^{-5} (long dash–dot). The tendency for the data to cross the model lines at low V_{rot} shows that some star formation took place during dissipational collapse of the Galaxy.

responds to that of an isothermal spheroidal distribution with a power law having index ~ -4.5, or to an exponential disk with scale length ~ 3 kpc. The tendency for the tracer populations with the lowest mean rotational velocities to have larger radial velocity dispersions than would be consistent with this density profile is of considerable significance, if real. We note that systematic distance uncertainties move the data roughly parallel to the body of the data with smaller σ_{rr}, so they are unlikely to be relevant.

With the exception of the data for the metal-poor RR Lyrae stars, however, there are very few stars in the bins with the highest values of σ_{rr}. The stars with the highest radial velocity dispersions are also the most metal poor (see below) and hence are those that presumably formed first in the Galaxy. If they really do form a more extended spatial distribution than more metal-rich stars, as suggested by Figure 3, then one may conclude that these stars formed from less dissipated gas and hence preserve a fossil record of the star formation and dissipation history of the proto-Galaxy during its first condensation from the expanding background. That is, there is a shallow *radial* abundance gradient in the Galactic spheroid but no evidence for a *vertical* abundance gradient. The lack of any increase of rotation velocity for metal-poor stars during the collapse may reflect angular momentum transport during spheroid formation, as evident in the *N*-body simulations of Zurek et al. (1988). Alternatively, it may be that the gas that formed stars more metal poor than ~ -1.5 dex had simply not collapsed by a sufficiently large factor to have acquired a measurable mean rotation velocity.

Although the asymmetric drift arguments above provide strong evidence that star formation continued *during* a period of dissipational collapse, there is no information in this relation regarding the *rate* of this collapse. For this, one requires another clock, which is provided by the chemical abundances.

3.2 *Correlations Between Kinematics and Chemistry*

Stellar chemical abundance is a clock that measures age in units defined by the formation rate and lifetimes of those (mostly massive) stars that contribute to the enrichment of the ISM. The mean azimuthal streaming motion $V_{\rm rot}$ of a population of stars reflects both the amount by which the proto-Galaxy dissipated and collapsed and the amount of angular momentum transport that occurred prior to the formation of these stars. Thus, the existence of a correlation between kinematics, such as $V_{\rm rot}$, and [Fe/H] allows one to relate the chemical evolutionary time scale to the dynamical and cooling time scales.

The existence or otherwise of an abundance gradient in the spheroid is often cited as an important diagnostic of the time scale of Galaxy formation, in the sense that the lack of a gradient is taken to mean a slow and/or chaotic collapse (cf. Searle & Zinn 1978, Carney et al. 1989b), and the presence of a gradient (manifest by a smooth correlation between kinematics and metallicity) to mean a rapid collapse (Sandage 1987a). In general, neither deduction need be correct, since although the presence of an abundance gradient means that dissipation was an important process during formation of the stellar component of the spheroid, this does not

necessarily define time scales. In a dissipationless collapse there is no arrow of time in the kinematics, and so no correlation between kinematics and metallicity. In a dissipative collapse, however, a star-forming gas cloud will be continually transferred onto lower energy orbits with time and will be successively enriched with time owing to continuing star formation. This creates a correlation between chemical abundance and orbital energy, which is an abundance gradient. Only low-metallicity stars will be found in the outer regions of galaxies that formed dissipatively, and high-metallicity stars will be found only in the inner regions.

However, since the cooling time of a proto-galaxy may be expected to be less than the free-fall collapse time (cf. Section 1), dissipation need not slow a collapse significantly. In a rapid (free-fall) dissipationless collapse no abundance gradient will arise, although one present in the initial conditions may survive, since violent relaxation in practice never goes to completion, as noted above. A slow dissipationless formation of the spheroid could occur if the field stars originated in many independent "fragments" that were captured and disrupted over a Hubble time (cf. Searle & Zinn 1978), with each fragment having its own star formation history. This last model would also not lead to an abundance gradient, owing to the assumed randomness of the "fragments." However, consideration of the element ratios of spheroid stars, as discussed in Section 3.4, poses stringent constraints on such a model for formation of the field stars. It may remain viable for the formation of the outer parts of the globular cluster system, as originally motivated.

Correlations (or the lack thereof) between the angular momentum of a tracer population of stars and the stars' chemical abundances, however, remain one of the most powerful observationally feasible tests of the early star formation and dynamical history of the Galaxy.

The amplitude of the peculiar velocity of a star also may be expected to be correlated with that star's metallicity. Since this peculiar velocity is now manifest in the star's orbital eccentricity, the relationship between the eccentricity of stellar orbits, projected onto the plane of the Galaxy, and chemical abundance is also commonly discussed. The general arguments above may be applied in support of its use. In addition to the uncertainties arising from the potential effects of violent relaxation, an extra note of caution is required in its interpretation, however. Unless one is confident that the levels of substructure in the proto-Galaxy and the consequent interactions (more precisely, the hydrodynamics of the dissipational and heating processes during Galactic collapse, and the mixing of the hot stellar ejecta into the infalling gas) are clearly understood, then one should not be entirely confident of the evolution of the *random* motions of newly forming stars.

3.2.1 ROTATION VELOCITY VS. METALLICITY The direct correlation between stellar chemical abundance and Galactic rotational velocity was first convincingly established and discussed in detail by ELS. An extensive debate has arisen in the past few years as a result of several new surveys of the kinematics of metal-poor stars, with conflicting claims as to the reality of this correlation for stars more metal poor than ~ -1 dex (Norris et al. 1985, Sandage & Fouts 1987, Sandage 1987a, Norris 1987a, Carney et al. 1989b, Norris & Ryan 1989b).

The relevant recent data are collected in Figures 4*a* and 4*b*. The agreement between the various data sets is acceptable for present purposes for stars more metal poor than ~ -0.8 dex. (Higher abundance stars are discussed separately below.) The mean value of the rotation velocity decreases from ~ 160 km s^{-1} at [Fe/H] $= -0.8$ to near zero at [Fe/H] $= -1.5$ and shows no significant correlation at lower abundances.

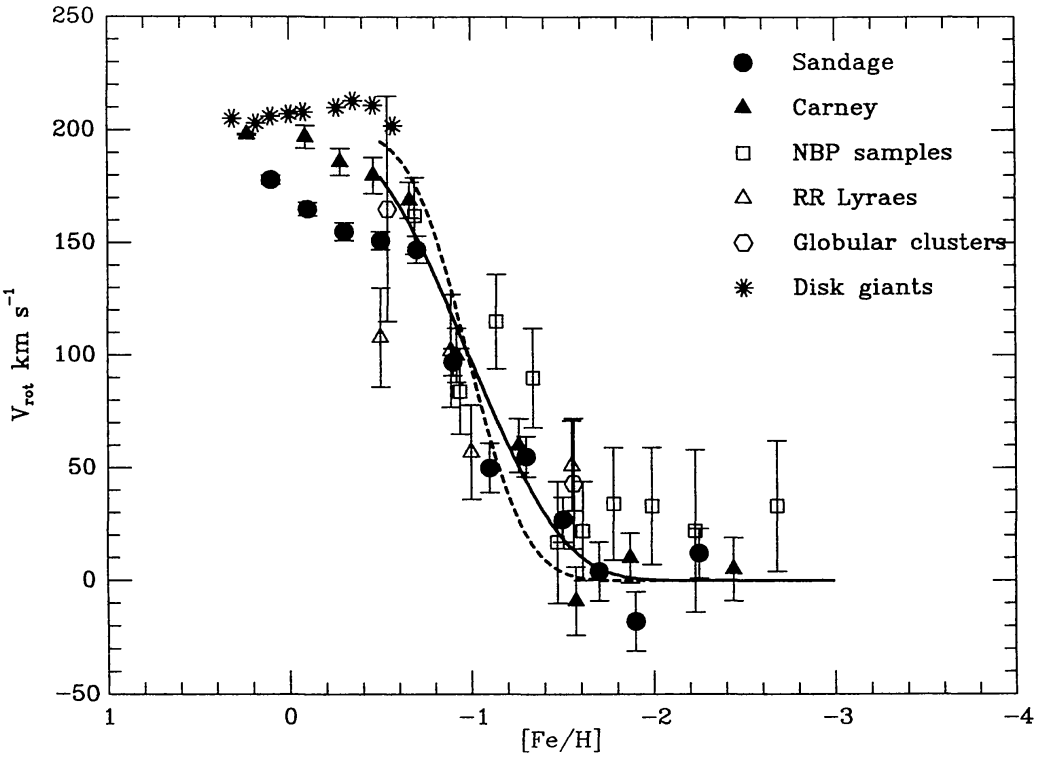

Figure 4a The relation between rotation velocity relative to the Galactic standard of rest (V_{rot}) and metallicity for those samples of field stars with good abundance data from Figure 3 and including the analysis of the disk globular cluster system by Armandroff (1989). The lines show alternative models; the solid line is a model involving a smooth correlation between V_{rot} and [Fe/H] over the range $-1.5 \lesssim$ [Fe/H] $\lesssim -0.5$. The dashed line shows a discontinuous relationship between V_{rot} and [Fe/H], with the discontinuity at [Fe/H] $= -1.0$. Both models have been convolved with a Gaussian of dispersion 0.25 dex in metallicity to represent measuring errors.

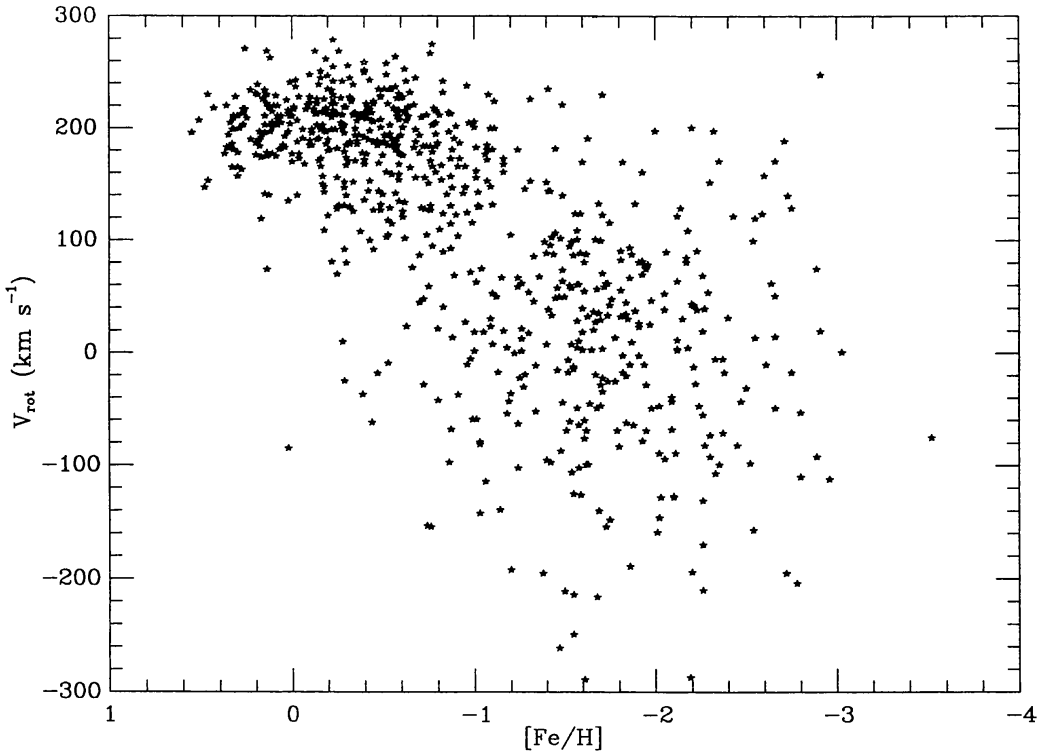

Figure 4b The relation between rotation velocity relative to the Galactic standard of rest, V_{rot}, and metallicity for the sample of proper-motion stars studied by Laird et al. (1988a). Comparison of this figure with Figure 4*a* illustrates the difficulty in deducing the reality of a smooth correlation between kinematics and metallicity from data that are averaged into bins, particularly for metallicities near −1 dex.

Above a metallicity of ~ -1.5 dex, there is a transition to a mean rotational velocity of $\gtrsim 160$ km s^{-1} at ~ -0.8 dex. These latter values are evidently very poorly determined. Is there a systematic abundance-kinematic correlation in the interval $-1.5 \leq$ [Fe/H] ≤ -1.0? While this may seem such a narrow abundance interval as to be unimportant, it in fact contains about one half of the stellar mass of the spheroid. The answer to this question is confused by questions concerning the precision of the data and the validity of binning data with such a large and asymmetric scatter as a function of abundance (Figure 4*b*).

The two curves shown in Figure 4*a* are, in turn, a linear correlation between ($V_{rot} = 0$ km s^{-1}, [Fe/H] $= -1.5$) and ($V_{rot} = 200$ km s^{-1}, [Fe/H] $= -0.5$) (solid line) and a discontinuity between $V_{rot} = 0$ km s^{-1} and $V_{rot} = 200$ km s^{-1} at [Fe/H] $= -1$ (dashed line). Both curves have been convolved with a Gaussian of dispersion 0.25 dex in [Fe/H] to illustrate the effect of measuring errors. The greatest uncertainty in distinguishing between the models is now the systematic differences between the results from different data sets. The spectroscopically selected samples discussed

by Norris et al. (1985) have a systematically higher rotation velocity than do the kinematically selected samples, for reasons that remain to be clarified. Nevertheless, the smoothed correlation is a slightly better description of the binned data than is the discontinuous model.

Sandage & Fouts (1987) interpreted their data as supporting the continuation of a smooth correlation between kinematics and abundance for *all* metallicities. It is clear from Figure 4*a* that there is no statistically significant difference between their sample and that of Norris et al. (NBP data points in the figure). Rather, the differences between the conclusions of the two groups result largely from different ways of binning data, which are clearly (Figure 4*b*) not adequately described by a mean and a standard deviation. One must discuss the distribution function of abundance and kinematic data to derive reliable conclusions. Fortunately, thanks to the very considerable efforts of Sandage & Fouts, Norris, and Carney & Latham, a sufficiently large and reliable data base is available for the first time to allow such a discussion.

One important conclusion from the discussion earlier in this section that is not widely appreciated is that the absence of a clear correlation between rotation velocity and metallicity at very low abundances does *not* mean that a rapid collapse model of the Galaxy is invalid. Thus, the conclusions reached by Sandage & Fouts (1987) are not incompatible with the data, even though their description of the data is not consistent with the appearance of Figure 4*a*. We emphasize that the presence or absence of such a correlation does *not* distinguish between fast and slow collapse models of the Galaxy. One may learn something about a complex combination of the importance of dissipation and the efficiency of violent relaxation, but time scales enter the interpretation of the relationship between rotation velocity and stellar metallicity only by assumption.

3.2.2 CORRELATIONS VS. DISCONTINUITIES A question of some interest is whether or not the appearance of Figure 4*b* is consistent with a continuous trend (indicative perhaps of significant star formation *during* the period when the proto-Galaxy was collapsing and spinning up) or instead represents a superposition of relatively discrete subsystems (indicative perhaps of the later merger of subsystems that retained a recognizable identity during the early stages of Galactic formation). Some suggestive but not conclusive evidence in favor of the picture of discrete substructure in phase space comes from the existence of several apparently intermediate groups of tracers that are identifiably discrete using astrophysical criteria. These include the metal-rich RR Lyrae stars ($\Delta S \lesssim 3$, $V_{\rm rot} \sim 110$ km s^{-1}; Strugnell et al. 1986), *c*-type RR Lyrae stars ($V_{\rm rot} \sim 100$ km s^{-1}; Strugnell et al. 1986), long-period variables with period between 150 and 200 days

($V_{rot} \sim 115$ km s^{-1}; Osvalds & Risley 1961), the metal-rich (G-type) globular clusters ([Fe/H] $\gtrsim -1$, $V_{rot} \sim 100$–200 km s^{-1}; Armandroff 1989), and the Arcturus moving group ($V_{rot} \sim 110$ km s^{-1}; Eggen 1987). The field type-II Cepheids (Harris 1981) are another closely related tracer sample, but they have less well-known kinematical properties at present.

It is remarkable that these different samples of objects all have almost exactly the same rotation velocity. Within the more considerable uncertainties, they also have similar abundances, $-1 \lesssim$ [Fe/H] $\lesssim -0.5$. [It was partially the similarity of this abundance range to that of the thick disk that motivated the suggestion by Wyse & Gilmore (1986) that the rotation velocity of the thick disk would also be ~ 100 km s^{-1}, lower than the angular momentum range compatible with recent data (see Section 4)]. Progress in understanding the amount of structure in the phase space distribution of old stars is most likely to follow further study of the Arcturus moving group, which, if a real and coeval feature in phase space, contains more new information about the dynamical evolution of the Galaxy than any other currently identified tracer population. The existence of such fine structure in phase space would require considerably more careful dynamical analyses of kinematic data (a "bowl of spaghetti" or "can of worms" model) but would also explain a variety of marginally significant observational phenomena that are otherwise inexplicable, such as the retrograde globular clusters (Rodgers & Paltoglou 1984) and field stars (Norris & Ryan 1989b) and the metal-poor moving groups (Eggen 1987, Sommer-Larsen & Christensen 1987). It is quite possible that a substantial fraction of the metal-poor stars now in the Galaxy were not formed there.

3.2.3 ORBITAL ECCENTRICITY VS. METALLICITY There is an alternative presentation of the relationship between stellar orbital properties and chemical abundance that is widely discussed. It involves the eccentricity of the stellar orbit in the Galaxy, projected onto the plane, and the star's metallicity. This presentation really depends on the ratio of the components of the star's velocity radially along and tangential to the line toward the Galactic center and on the stellar metallicity. The derivation of an orbital eccentricity requires the additional assumption of a Galactic potential, which adds further uncertainty. Nevertheless, the existence of a correlation between metallicity and the shape of the stellar orbit projected onto the plane of the Galaxy has been cited as the principal evidence leading ELS to support a rapid collapse model of the Galaxy (Sandage 1987a). Similarly, observational evidence that a tight correlation is violated by a significant fraction ($\sim 20\%$) of field metal-poor stars has been cited as evidence that a slow collapse is a preferred model (Yoshii & Saio 1979, Norris et al. 1985). This correlation is therefore worthy of explicit discussion.

The observational status of such a correlation is a little confused at present. The large kinematically selected samples studied recently by Sandage & Fouts (1987), Laird et al. (1988a), and Norris & Ryan (1989a) are naturally biased against stars with nearly circular orbits, as such stars will (owing to the trade-off between the various terms in Equation 12) tend to have smaller peculiar space velocities than stars on lower angular momentum orbits with the same total energy. Thus careful modeling of the available data will be required to test that any correlation between orbital planar eccentricity and stellar chemical abundance is not due to a selection bias. Low-abundance stars are intrinsically sufficiently rare, and those with both sufficiently large peculiar velocities to enter a kinematically selected sample and the correct angular momentum to reach the solar neighborhood occupy such a tiny fraction of the whole of phase space that one would not expect to find them readily in any case. Low-metallicity stars on nearly circular orbits may well exist in very large numbers nearer the Galactic center, irrespective of the rate of star formation during collapse of the Galaxy.

We emphasize that what is really at issue is the existence or otherwise of a significant number of stars with low metallicities, high angular momenta, and small peculiar velocities. These stars are further discussed in Section 4 under the guise of the "metal-poor thick disk." In the ELS rapid collapse picture, stars acquire large systematic rotation velocities (random velocities are ascribed to initial conditions) owing to the spin-up of the proto-Galaxy as it collapses, with conservation of angular momentum. Thus, mean rotational velocity is a direct measure of the collapse factor of the star-forming gas (if viscosity is unimportant) and is therefore a clock for the collapse, in the same way that stellar abundance is a clock for star formation. Since the natural time scale for an increase in rotational velocity due to Galactic collapse is a free-fall time, ELS deduced from their observed orbital shape–abundance correlation that star formation also occurred on a free-fall time scale. The basic rapid-collapse model of ELS assumes that star-formation, chemical enrichment, and collapse proceed at the same time, so that, in their model, one would not expect to find a substantial number of stars that are metal poor (i.e. among the first stars formed according to the chemical clock) but on roughly circular orbits (i.e. among the later stars formed according to the collapse clock). The ELS model would allow a substantial number of metal-poor stars with both high angular momentum and high orbital energy, as ELS have emphasized. Such stars would, however, still be on eccentric orbits (cf. ELS's discussion of their Figure 9 for this point).

Since there do exist some stars with low metallicity on nearly circular orbits (Norris et al. 1985, Norris 1987a), does this rule out the rapid

collapse model, and does it support a slower collapse alternative? To answer these questions, one must rediscuss the important assumptions behind the argument (cf. Section 1.2). For present purposes, these are that the collapse was synchronized, so that metal enrichment follows the collapse factor locally (equivalently, the collapse clock and the enrichment clock are in phase everywhere, with a similar time scale for the two processes—this is necessary, since no correlation would be seen if the two time scales were very different); that the Galactic gravitational potential changed slowly at all times; and that the concept of a "gas cloud" retaining kinematic parameters during the collapse and enrichment process up to formation of a low-mass star is reasonable.

Since the correlation of orbital eccentricity and metallicity discussed by ELS is apparently violated by many stars, a variety of possibilities arise. Searle & Zinn (1978) developed a model in which the synchronization of the collapse and enrichment clocks was put out of phase by allowing the existence of substantial substructure, which survived as gravitationally bound entities for longer than a Galactic collapse time. In effect, their model is a sum of a large number of small ELS-like collapses, but with a different *rate* of enrichment (equivalently, star formation) in each element. [The most useful constraints on models of this type come from cooling-time arguments (cf. Section 1.1) and from study of the relative enrichment rates of different chemical elements, which provides a higher temporal resolution clock. Such constraints are discussed further below.] An alternative possibility has been suggested by Norris (1987a)—that the time scale for the Galactic collapse was much longer than a dynamical time scale, though it is not clear how this model can be consistent with the data either. The Larson (1976) model that Norris utilizes as an example predicts smooth, steep, vertical metallicity gradients. Merely changing the absolute time scale (in years) of both the collapse and the star formation rates will, of course, have no effect on the predictions of the ELS model if both rates are changed proportionately, since neither has been formulated in years. Although hydrodynamical support of the gas against collapse might well act to damp out random motions in the gas clouds during a slow collapse, this possibility on its own is not consistent either with the observations or with the cooling time scale arguments of Section 1.1. Clearly, changing the relative rates of the collapse and enrichment will change the *slope* of any resulting correlation, but it will not change the scatter. It is increased scatter that must be explained. Such scatter can be explained (under the assumptions that chemical abundance is a monotonic clock and that violent relaxation has not erased the fossil record) by inhomogeneity in either the chemical enrichment rate or the gaseous collapse factor (Searle & Zinn 1978), or by a wide diversity in the distribution of initial (precollapse)

angular momenta among gas clouds, but not by merely changing the rapidity of the proto-Galactic collapse. The absence of a tight correlation between orbital eccentricity and metallicity does not support a slow collapse model of the Galaxy and in fact argues against a slow, dissipative collapse.

Perhaps the most important feature of the eccentricity-metallicity relation is that stars on highly radial orbits exist at all. A star can now be on a radial orbit either simply because it has dropped out of the quasi-static collapse of a pressure-supported gaseous Galaxy, or because it formed from gas that was on a highly radial orbit—and that would be undergoing rapid collapse owing to the cooling-time arguments—or because it formed on some other orbit that was subsequently made more radial by violent relaxation. The first alternative, which was not considered feasible in principle by ELS, is in fact ruled out by the lack of a steep abundance gradient in the metal-poor spheroid, as discussed above. The remaining two mechanisms involve rapid collapse of something—either the spheroid itself or the dominant mass of the Galaxy, which is not the spheroid. Thus, the combination of kinematic and chemical data implies that the existence of a significant number of subdwarf stars on radial orbits requires a rapid collapse of the spheroid and/or the dominant contribution to the mass of the central few kiloparsecs of the Galaxy.

Similarly, in a rapid collapse model one also expects any *tight* correlation that might have existed between stellar kinematic parameters and time-independent internal properties of the star (e.g. chemical abundance) to be smeared out by the violent relaxation. That is, contrary to the expectation of ELS [who it must be emphasized were working before the discovery of the concept of violent relaxation, by L (Lynden-Bell 1967b)], one does *not* expect a strong correlation of orbital eccentricity and metallicity in a rapid collapse model. The existence of a large fraction of spheroid stars on highly radial orbits at all is strong evidence for rapid collapse of most of the mass of the Galaxy, but it does not of course provide any evidence for determining whether or not the formation of most spheroid stars was completed before, or took place during, the collapse of the dominant contribution to the mass of the Galaxy.

3.3 *Correlations Between Abundances and Ages*

Calibration of the abundance enrichment rate onto a time scale that is calibrated independently of the collapse rate (i.e. in years) is necessary to provide direct evidence for the time scale of Galactic formation. In practice, only stars near the main-sequence turnoff have surface gravities that change sufficiently rapidly and monotonically that reliable comparison with evolutionary tracks is possible, although some useful information on a combination of age and chemical abundance can be derived from the

color of field giant stars (e.g. Sandage 1987a). For *single* stars near the turnoff, the comparison of *uvbyβ* photometry with theoretical isochrones is by far the most reliable and precise age-dating technique available. If independent abundance estimates are available, then any photometric measure of the temperature of the hottest turnoff stars will measure the age of the *youngest* star in a tracer population. It is this method that is utilized to determine ages for globular clusters, where it also seems that all the member stars are coeval. A similar technique can be applied to field stars (cf., for example, Gilmore & Wyse 1987) and is illustrated in Figure 5. This figure shows the color-metallicity data for the high-proper-motion stars studied by Laird et al. (1988a), as well as the turnoff points of all those globular clusters with recent CCD photometry, and a representative isochrone for old metal-rich stars (VandenBerg & Bell 1985).

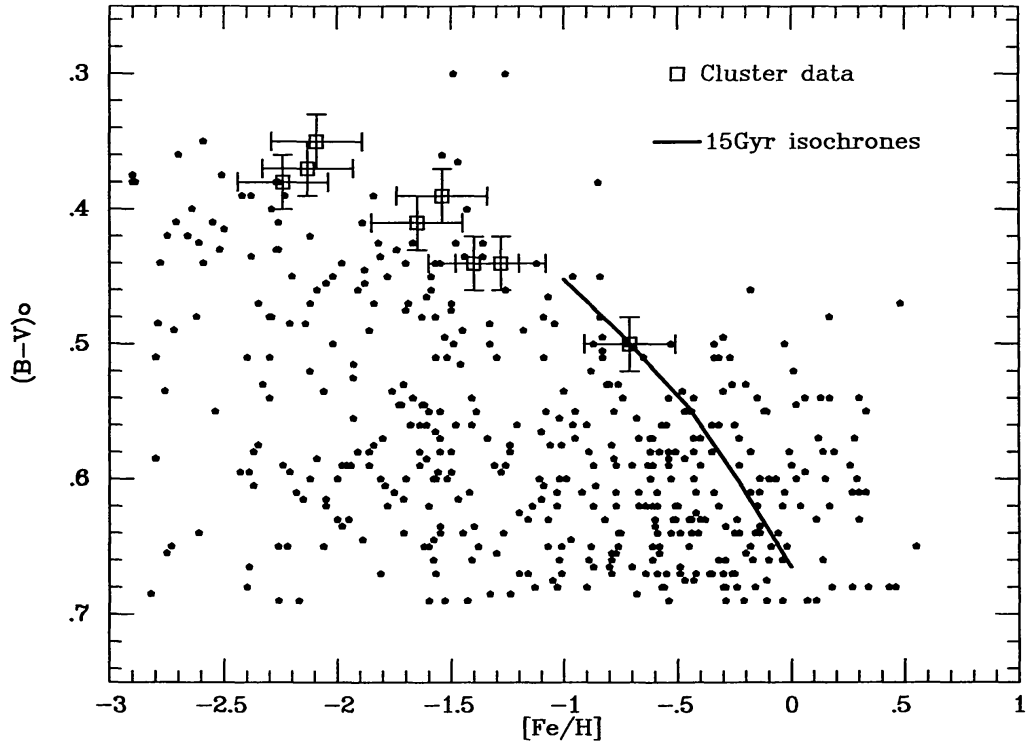

Figure 5 The $B-V$ vs. [Fe/H] relation for all stars observed by Laird et al. (1988a; points) and for those globular clusters with turnoff colors from recent CCD photometry (Stetson & Harris 1988; boxes). The photometric data are corrected for interstellar reddening. The solid line is a 15-Gyr isochrone calculated with oxygen-enhanced element ratios and scaled in $B-V$ to match the turnoff color of 47 Tuc. The blue edge of the stars with [Fe/H] $\lesssim -0.8$ is adequately defined by the isochrone and by the globular cluster data, which shows that effectively all stars more metal-poor than ~ -0.8 dex are as old as the globular clusters. At higher abundances, the trend for the data to move to the blue of the isochrone shows that at least some stars are younger than the globular clusters.

The important conclusion from Figure 5 is that essentially all stars with [Fe/H] $\lesssim -0.8$ are, insofar as is measurable, the same age as the globular cluster system. [Note, however, that Schuster & Nissen (1989) suggest that there is a real age spread of ~ 3 Gyr in the subdwarf system and even possibly an age-abundance relation in metal-poor stars. This time scale is much longer than those deduced in other ways and will radically alter our perception of Galactic evolution, if real. It deserves considerable attention.] Stars more metal rich than ~ -0.8 dex have a bluer turnoff, which implies that *at least some* of these stars are younger. The *distribution* of ages is, however, unmeasurable from a turnoff color. Some information on the age distribution for stars with [Fe/H] $\gtrsim -0.8$ is provided by studies of open clusters. These form a system with a very large scatter in the age-metallicity plane; for example, clusters exist near the Sun with solar abundance and an age of 12 Gyr (NGC 6791; Janes 1988), and with [Fe/H] ~ -0.5 but an age of only a few gigayears (e.g. Melotte 66). A similar scatter is evident in the age-metallicity relationship for F-dwarfs near the Sun (Twarog 1980, Carlberg et al. 1985, Knude et al. 1987), though unfortunately both qualitative and quantitative differences are found from author to author (even analyzing the same sample), which somewhat confuses the real situation. Thus, any attempt to deduce a representative age for a stellar population from the turnoff color of the *bluest* field stars with metallicity $\gtrsim -0.8$ dex (Norris & Green 1989) is fundamentally unreliable. This point is returned to in Section 4 below.

3.4 *Chemical Element Ratios and Galactic Collapse*

One of the most important constraints on the homogeneity of star formation in the spheroid, and hence on chemical evolution, is readily derivable from the observed small dispersion in the position of the breaks in element ratios as a function of [Fe/H]. As we show below, the inferred lack of cosmic scatter implies little spatial variation in the star formation history of the proto-Galaxy, which is obviously of considerable importance in determining the levels of independent substructures in the gas cloud that became the Galaxy. Models such as those of Searle (1977; Searle & Zinn 1978), whereby the spheroid is a result of the merging of many independent "fragments," each with its own chemical enrichment history, seek to explain the entire range of metallicity seen in halo stars as being due to the statistical effects of chemical inhomogeneities, rather than as a trend with age. The "fragments" are assumed to be disrupted by some process after some time, producing the field stars of the halo (cf. Fall & Rees 1977). Such models also predict a large spread in the element ratios observed from field star to field star if, for any one of the "fragments" (each of which is presumed to contain many globular cluster–sized objects),

star formation continued for sufficiently long that Type I supernovae became a significant source of iron.

At metallicities above ~ -1 dex, the [O/Fe] ratio declines toward the solar value (see Figure 1). The slope of this relation is ~ -0.5 (thus the iron is mimicking the behavior of a "secondary" element), which implies that the amount of iron synthesized in association with oxygen is small compared with the amount synthesized independently of oxygen. This must hold even though the relevant [Fe/H] range encompasses the entire thick disk and most of the thin disk. We may utilize this constraint to determine the relative rates of Type I and of Type II supernovae during the epoch of formation of the disks, which in turn constrains the star formation rate during the formation of most of the stellar mass of the Galaxy. If we assume a constant initial-mass function (IMF), the star formation rates in the thick and thin disk formation stages must be low enough to prevent imprinting a feature through their associated massive stars. Assuming that single stars more massive than 8 $M_\odot$ explode as Type II supernovae, and that binary systems with a minimum primary mass of 5 $M_\odot$ eventually evolve into Type I supernovae, integration of the Miller & Scalo (1979) IMF predicts that the number of potential progenitors of Type I supernovae is a factor ~ 1.5 higher than the number of progenitors of Type II supernovae. The time for an individual star to become a supernova depends sensitively on the initial orbital properties and could easily be several Hubble times. The rate of Type I supernovae is therefore impossible to predict analytically. Observations of the present relative rates of Type I and Type II supernovae offer the most reliable constraint. Tammann (1982) finds that the Type I : Type II ratio is $\sim 1.5:1$ in a range of spiral types (Sab–Sd). Such galaxies have derived average star formation rates that vary little over the past $\sim 6 \times 10^9$ yr (Gallagher et al. 1984), despite differences in gas content and metallicity. Thus the present relative rates of Type I and Type II supernovae in disk galaxies may be assumed to be roughly constant over a large fraction of a Hubble time, and most potential candidates for Type I supernovae actually explode in less than a Hubble time.

Current models agree that each Type I event ejects ~ 0.6 $M_\odot$ of iron (e.g. Woosley & Weaver 1986), although there is less consensus about the yield from Type II supernovae, partly because of the uncertainties in how much of the progenitor envelope is actually ejected unchanged. The bare-core calculations of Arnett (1978) produced only ~ 0.25 $M_\odot$ of iron for stars of main-sequence mass $20 \lesssim (M/M_\odot) \lesssim 30$, assuming that 60% of the "Si" yield is ejected as iron and adopting his transformation between core and main-sequence masses. Woosley & Weaver (1986) find about a factor of two more iron than does Arnett for their standard 25-$M_\odot$ model.

Here we assume that each Type I event yields a factor of two more iron than every Type II event (0.6 $M_\odot$ and 0.3 $M_\odot$, respectively). The observation that current rates, averaged over a range of spiral galaxies with fairly constant star formation rates, are $\sim 1.5:1$ for Type I : Type II implies that roughly three fourths of the iron production averaged over the lifetime of the Galaxy is from Type I events. Thus, adopting an oxygen yield of 0.6 $M_\odot$ for each typical Type II event (Woosley & Weaver 1986) and the iron yields above implies that 1.2 $M_\odot$ of iron and 0.6 $M_\odot$ of oxygen, or twice as much iron as oxygen, are returned to the interstellar medium per unit time. The return of fixed amounts of iron and oxygen, rather than fixed increments, of course results in the prediction of a nonlinear slope to the [O/Fe] : [Fe/H] relation. As shown in Figure 1, the observations are well fit by this prediction, which suggests that the star formation rate has indeed been fairly constant over the lifetime of the disk and perhaps supports Tammann's *relative* supernovae rates. It must be noted, however, that the uncertainties in the supernova yields and in the observed supernova rates are so large that no unique model exists. The relative supernova rates of van den Bergh et al. (1987) (Type I : Type II $\sim$ 1:1.5), where we have added together the Type Ia and Type Ib supernovae, would lead to approximately equal amounts of iron from each type of supernova, and equal amounts of iron and oxygen returned to the ISM per unit time, if we assume naively that both Type Ia and Type Ib have the same yield of iron. The enhanced rate of Type II supernovae leads to a predicted relation between [O/Fe] and [Fe/H] that has a less steep initial decay than that obtained using Tammann's (1982) relative rates, but that is also consistent with the observations owing to their large scatter.

The explanation, reiterated above, of the breaks in element ratio as a function of [Fe/H] as simply reflecting different element production sites depends on the existence of a simple correspondence between [Fe/H] and time. However, this mapping depends on the star formation rate and the stellar IMF. If we assume the IMF to be constant, "fragments" of higher star formation rate will have attained a higher [Fe/H] prior to the fixed time at which Type I supernovae dominate, so that the break in the [O/Fe] : [Fe/H] relation will occur at higher [Fe/H]. Similarly, "fragments" of substantially lower star formation rate would lead to a break at much lower [Fe/H]. Thus, samples of stars that originated in many different "fragments" that were subsequently disrupted would not show a well-defined break at one given metallicity, contrary to the observations. The small scatter seen then requires that all "fragments" had evolved to nearly the same gas fraction at the time when they were disrupted, which in all cases was $\lesssim 10^9$ yr after significant star formation began. Such an effect is implicit in the models of Hartwick (1976) and Gilmore & Wyse (1986),

whereby the metallicity distribution of the extreme spheroid is a consequence of gas being lost from the star-forming process at a rate proportional to, and greater than, the star formation rate. The required rate of gas removal is a factor of 10 to 15 higher than the star formation rate, so it is possible for each "fragment" to evolve to completion (by losing all its gas) in a time shorter than that required by the break in the [O/Fe]:[Fe/H] relation (or $\lesssim 10^9$ yr).

"Fragment" models also require that star formation began over all of that part of the proto-Galaxy that became the extreme spheroid in the solar neighborhood at nearly the same time. This requirement arises because if some "fragments" lagged behind and began their chemical evolution substantially later than most, their oxygen-rich ejecta would have enriched the gas that was to form the younger disk populations, contrary to the observations. A further constraint on the spatial variations of the star formation process in the spheroid comes from the fact that metals may be transported at no more than the local sound speed, whereas the free-fall velocity may well be supersonic for an ISM at about 10^4 K (Fall 1987), which would lead to large local chemical inhomogeneities if the star formation rate varied rapidly from place to place. However, if the gas has been heated to the Galactic virial temperature, the sound speed will equal the free-fall velocity, by definition, so that efficient mixing is not constrained by the distance ejecta can be transported in a free-fall time. In general, it seems more plausible to identify any "fragments" with short-lived condensations that become the sites of star formation in a gaseous background, rather than as discrete structures merging to form the proto-Galaxy. The existence of structure in the element ratio relations is strong evidence that there was a continual increase with time of the heavy-element abundance of the Galaxy up to the time when the metallicity reached that at which the relations change slope, and it is difficult to reconcile with stochastic chemical evolution models.

3.5 *The Time Scale of Galaxy Formation*

In view of the complexity of the discussion above, we provide here a brief summary of the observational constraints on the time scale over which the extreme Population II stars in the Galaxy formed. The most important observational constraint is provided by the constancy of the oxygen-to-iron element abundance ratio as a function of iron abundance for metal-poor stars (Section 1.3). These data show the stars in the Galaxy with metallicities less than ~ -0.8 dex to have formed on a time scale of $\lesssim 1$ Gyr. Analysis of the asymmetric drift data (Section 3.1) shows that the most metal-poor stars formed during a period of dissipational collapse of unconstrained duration. Study of the correlations between stellar kine-

matics and stellar metallicities (Section 3.2) shows that the stars that formed during the dissipational collapse are the subset with metallicities $\lesssim -1.5$ dex of the same stars whose age range is set by the oxygen-to-iron element ratios. It is not yet clear if the apparent absence of evidence for dissipation during formation of the more metal-rich spheroidal stars [that is, the lack of a detectable abundance gradient (Section 3.2)] indicates that the dissipational collapse had effectively ceased, or at least had become dissipationless, during their formation. It may well be simply that a subsequent period of violent relaxation of the Galactic potential well has disturbed the fossil record of the state of collapse of the proto-Galaxy during the formation of the more metal-rich extreme Population II stars. Since a characteristic time scale for dynamical evolution is ~ 0.5 Gyr (Section 1.1), one may deduce that the period of star formation leading to the present extreme Population II stars occurred during a dissipational collapse that lasted for no more than a few dynamical times. Hence, the Galaxy formed its first generations of stars during a period of "rapid" (cf. Section 1.1) collapse. Further constraints on the homogeneity of the proto-Galaxy during this collapse are discussed in Section 3.4.

4. THE THICK DISK

The luminosity profile of the Milky Way, as given by star counts, provides evidence for a Galactic thick disk, as discussed in Section 2.5. Indeed, recent photometric and spectroscopic stellar surveys have emphasized the importance of the intermediate Population II stars, as introduced at the 1957 Vatican Conference (Oort 1958, O'Connell 1958). The modern characterization of this population assigns to this stellar component a vertical scale height of ~ 1–1.5 kpc, a vertical velocity dispersion of ~ 45 km s^{-1}, a typical stellar chemical abundance of $\sim 1/4$ of the solar metallicity, and a mean asymmetric drift of ~ 30–50 km s^{-1}. The detailed values of the descriptive parameters remain poorly determined, however, primarily because the offset in the mean values characterizing the thick disk distribution function over age, metallicity, and kinematics from those mean values characterizing the oldest thin disk stars is much less than the dispersions in these quantities. Reliable determination of the parameters of the distribution function is important, since it may allow a discrimination between the several currently viable models of the formation of the thick disk.

Possible formation mechanisms for the thick disk include the following:

1. A slow, pressure-supported collapse phase following formation of the

extreme Population II system, similar to the sequence of events in Larson's (1976) hydrodynamical models of disk galaxy formation.
2. Violent dynamical heating of the early thin disk by satellite accretion (cf. Hernquist & Quinn 1989) or by violent relaxation of the Galactic potential (Jones & Wyse 1983).
3. Accretion of the thick disk material directly—for example, by satellite accretion with a preferential population of suitable orbits (Statler 1988).
4. An extended period of enhanced kinematic diffusion of stars formed in the thin disk to high-energy orbits (Norris 1987a).
5. A rapid increase in the dissipation and star formation rates due to enhanced cooling once the metallicity is above ~ -1 dex (cf. Wyse & Gilmore 1988).

Discrimination among these several types of models is possible from appropriate age, metallicity, and kinematic data. The first type of model noted above will lead to an intermediate-age system, with an abundance gradient. The second will have a small internal age range but is unlikely to have an extant abundance gradient (*modulo* the details of the dynamical evolution). The third has a wide variety of allowed combinations of age and abundance, while the fourth will have a range of ages, a similar chemical abundance to the thin disk, but a kinematic discontinuity between the old disk and the thick disk. The last model predicts that the thick disk will be kinematically distinct from the metal-poor spheroid and will have metallicity $\gtrsim -1$ dex. In view of this possibility to determine the evolutionary history of the thick disk, an extensive debate is underway to describe reliably the kinematic, abundance, and age structure of the thick disk (cf. Sandage 1987a, Norris 1987a).

Here we summarize the data on the determination of the chemical abundance distribution and the age range of thick disk stars, and we also discuss the difficult questions of the relationships among the stellar populations near the Sun.

4.1 *Metallicity of the Thick Disk*

As discussed in Section 3, the chemical abundance of a stellar population contains much information about the population's early evolution, while detailed information about vertical metallicity gradients can test the reality of discrete stellar populations (Sandage 1981). The metallicity distribution of stars in situ above the thin disk plane has been the subject of several modern spectroscopic and photometric surveys. A population with a vertical velocity dispersion of ~ 45 km s^{-1} will dominate samples of stars presently at z-heights ~ 1 to a few kiloparsecs if it comprises of order 1% of the stars in the Galactic plane. Hence, distances of ~ 2 kpc from the

plane are the most suitable environment to study the properties of the thick disk. Hartkopf & Yoss (1982) obtained DDO-photometric metallicity estimates for a spectroscopically selected sample of K giants at the Galactic poles; their data for stars with distances between 1 and 2 kpc are consistent with a Gaussian in log-metallicity, with mean $\langle[Fe/H]\rangle = -0.6$ and $\sigma_{[Fe/H]} = 0.3$ dex (Gilmore & Wyse 1985). This conclusion was confirmed by Yoss et al. (1987) for an augmented sample, though it should be noted that Norris & Green (1989) have reobserved many of the most metal-rich but distant Hartkopf & Yoss stars and conclude that both the distance and metallicity were overestimated by Hartkopf & Yoss. Norris & Green therefore suggest a revised, smaller dispersion for the thick disk metallicity distribution. The spectroscopically selected giant samples of Ratnatunga & Freeman (1985, 1989) and of Friel (1987, 1988) also contained relatively few metal-poor stars, in contradiction to the predictions of models that assume that the spheroid has metallicity similar to the metal-poor globular clusters. In particular, Friel's observations were in accord with the existence of a thick disk with scale height ~ 1 kpc and local normalization $\sim 3\%$, the stars of which have metallicity similar to the metal-rich globular cluster 47 Tuc (~ -0.7 dex). The kinematics of Ratnatunga & Freeman's stars is discussed further below (cf. also Freeman 1987).

The kinematically defined sample of Eggen (1979), when restricted to stars with vertical velocities $40 \lesssim |W| \lesssim 60$ km s^{-1}, has a metallicity distribution that is bimodal, with well-defined peaks at ~ -0.7 and -1.5 dex, in (remarkable) agreement with the globular cluster data of Zinn (1985). The metallicity distributions seen across other restricted velocity ranges are consistent with three discrete metallicity distributions for the metal-poor spheroid, the thick disk, and the thin disk, as are the proper-motion samples of Sandage & Fouts (1987) and Carney et al. (1989a). Distinct chemical abundance distributions for the thick and thin disks pose a problem for the fourth model of thick-disk formation briefly described above (scattering of extant thin-disk stars) and an embarrassment for the first model, where one expects smooth continuity.

This higher metallicity for the majority of spheroid stars than that implied by the solar neighborhood subdwarfs has important consequences for the chemical evolution of the solar neighborhood, and in particular for the "G-dwarf problem," which is the apparent lack of metal-poor, long-lived stars in the solar neighborhood compared with the predictions of the "simple closed-box" model of chemical evolution (van den Bergh 1958, 1962, Pagel & Patchett 1975). Whether or not the thick disk is a discrete entity is irrelevant here, since all that is of importance is that there exist G-dwarfs of metallicity ~ -0.6 dex that were not represented adequately in earlier surveys (cf. Yoshii 1984, Gilmore & Wyse 1986).

4.2 *Is the Thick Disk Kinematically Discrete?*

Here we address the kinematics of the thick disk—in particular, what one can infer about the evolutionary status of these stars from the similarities and differences of their kinematics from those of other populations in the Galaxy.

4.2.1 IS IT DISCRETE FROM THE SUBDWARF SYSTEM? The weighted mean average velocity dispersions for nonkinematically selected extreme Population II stars are determined to be $(\sigma_{rr})^{1/2}:(\sigma_{\phi\phi})^{1/2}:(\sigma_{zz})^{1/2} = 131\pm7:102\pm8:89\pm5$ (Carney & Latham 1986, Norris 1986, Morrison et al. 1989). The vertical velocity dispersion of the thick disk is $\sim$45 km s^{-1} [cf. Ratnatunga & Freeman 1985, 1989, Gilmore & Wyse 1987 (Figure 12*A*), Sandage & Fouts 1987, Yoss et al. 1987, Carney et al. 1989a]. The lag behind solar rotation (the asymmetric drift) of the thick disk is apparently 30–50 km s^{-1} (Ratnatunga & Freeman 1985, 1989, Freeman 1987, Norris 1987c, Sandage & Fouts 1987, Morrison et al. 1989), while that of the subdwarf population is 180–220 km s^{-1} (Norris 1986; cf. Section 3.2). Thus the kinematics of the thick disk is dominated by rotational support, while that of the subdwarf system is dominated by "pressure" support from the anisotropic velocity dispersion tensor. One explanation for this dichotomy is simply that the rate of dissipation in the vertical direction was relatively high, compared with the star formation rate, as the protodisk collapsed.

The number of stars with abundances and kinematics such that they might plausibly be assigned either to the low-velocity tail of the extreme Population II or to the high-velocity tail of the thick disk (i.e. those stars with [Fe/H] ~ -1) is very small. Figure 4*b* shows the *distribution* over rotation velocity and metallicity for the sample of Laird et al. (1988a); the binned data are shown in Figure 4*a*. It is clear that there is a relative deficiency of stars with [Fe/H] ~ -1 and -200 km $s^{-1} \lesssim V \lesssim -100$ km s^{-1}. However, this overlap region is populated; in particular Norris et al. (1985) drew attention to metal-poor stars with thick disk kinematics, while Morrison et al. (1989), from their spectroscopically selected sample of G/K-giants in a field against Galactic rotation, suggest that stars with "disk kinematics" (large rotation velocity) and stars with "halo kinematics" exist in approximately equal numbers with metallicities ~ -1 dex. Thus Morrison et al. characterize the binned rotation velocity vs. metallicity plot of Figure 4*a* as two vertically offset, horizontal lines that overlap in metallicity, rather than either the step-function or the smooth correlation considered in Section 3. The relation of these stars to the flattened metal-poor component found by Hartwick in the metal-poor RR Lyrae stars and in the metal-poor globular clusters (discussed in Section 2.6) is not

obvious, especially since Morrison et al. explicitly analyzed the kinematics of samples of RR Lyrae stars and of globular clusters and saw no behavior similar to that of their K-giants. The existence of a significant "metal-weak thick disk" obviously would have major ramifications for our understanding of the thick disk as a discrete entity; a few high-angular-momentum but metal-poor stars are predicted in many models of Galaxy formation, such as that of ELS, but these stars should be on highly eccentric orbits. Proper motions for the Morrison et al. sample would be highly desirable, as would the kinematics of similar samples of stars in fields that probe different components of the space motion. In this regard, Ratnatunga & Freeman (1985, 1989) interpret their K-giant south Galactic pole (SGP) data as consistent with only *one* metal-poor component, as do Yoss et al. (1987). Thus the situation remains confused, primarily as a result of the very small number of stars that might belong to such a metal-poor tail of the thick disk, and of the consequent difficulties in determining their properties and relationships to other groups of stars.

4.2.2 IS IT DISCRETE FROM THE THIN DISK? The relationship of the thick disk to the high-velocity tail of the old disk is equally problematic and has been discussed extensively by Sandage (1987a) and Norris (1987a). The main point at issue is whether there is a continuous relationship of vertical velocity dispersion with metallicity extending all the way to the $\sim$45 km s^{-1} vertical velocity dispersion of the thick disk, or whether the old disk velocity dispersion becomes asymptotically constant at the value of $\sim$22 km s^{-1} appropriate for spectroscopically selected samples of old dwarfs near the Sun (Fuchs & Wielen 1987, Sandage 1987b)? The deconvolution of *local* samples of proper-motion stars into components whose kinematics are similar (within a small multiplicative factor) to those of the old disk is fraught with difficulty. Preliminary attempts have been made (I. N. Reid & I. Lewis, private communication, 1988) to illustrate this uncertainty and to show that reliable results must await careful analysis of the several in situ surveys that are nearing completion.

The difficulty in deciding whether there is a continuous kinematic continuity from the thick disk to the old disk is illustrated by Figure 6*a*. This shows the vertical velocity distribution of those stars in the Gliese catalogue of nearby stars with photometric abundance parameter $\delta_{0.6} < 0.15$ ([Fe/H] $\gtrsim -0.9$; this abundance range was chosen so as to exclude high-velocity subdwarfs). The two models overlaying the histogram data are a two-component model, with discrete old thin disk and thick disk, and the four-component approximation to a continuous relation between the old disk and the thick disk fitted by Norris (1987a). The two models are clearly both excellent descriptions of the data, and they are equally clearly indistinguishable.

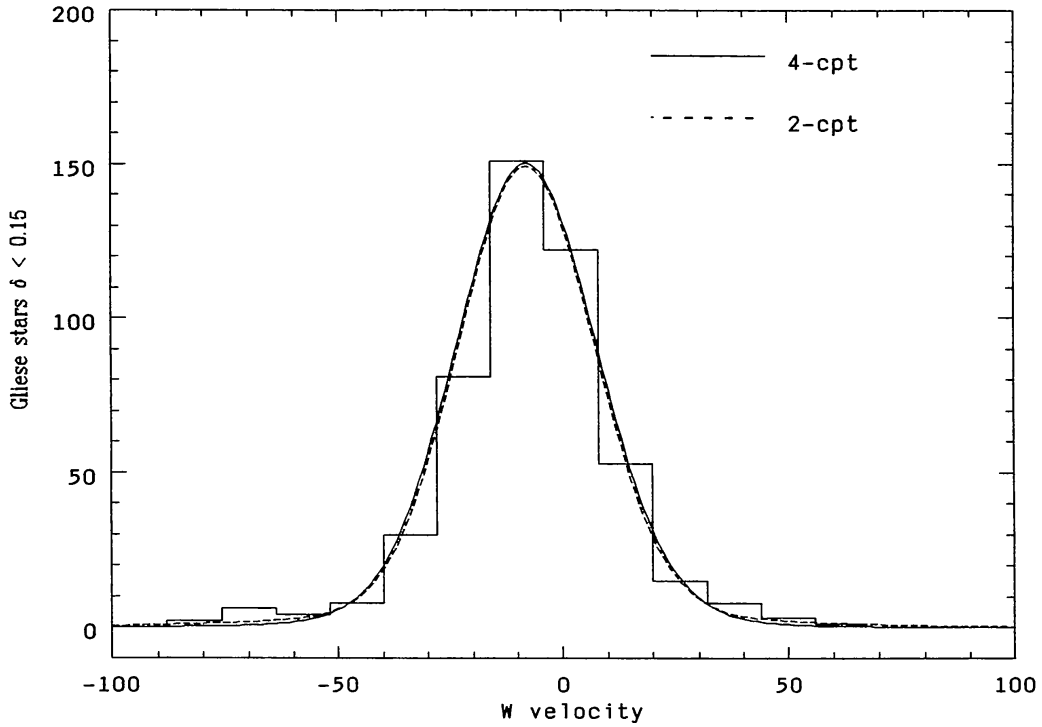

Figure 6a The distribution of vertical (W) velocities of stars in the Gliese catalogue, excluding stars with $\delta_{0.6} > 0.15$. The two lines illustrate models with a kinematically discrete thick disk (dashed lines) and with a continuous kinematic relationship between the old disk and the thick disk (solid line). Distinguishing between these models on the basis of these data is clearly not possible.

The data that motivated the four-component model are shown in Figure 6*b*, together with the data for the F-star sample of the Copenhagen group (Strömgren 1987). The important points to note here are the unsatisfactory disagreement between the two data sets, and the level of smoothness or otherwise of the observed trend.

It is evident from Figure 6 that available *local* data are incapable of determining if the old disk and the thick disk are kinematically discrete. Resolution of this uncertainty, with its important implications for the formation history of the Galaxy, must await completion of the several extant in situ surveys of the stellar distribution several kiloparsecs from the Galactic plane. The available data marginally favor a model in which the thick disk is a kinematically discrete component of the Galaxy, but the issue remains to be decided by observational test.

However, the theoretical predictions for how various secular scattering mechanisms act to increase the velocity dispersion of a population of stars as it ages are fairly clear. Scatterers that are confined to the plane of the Galaxy, such as giant molecular clouds (GMCs; Spitzer & Schwarzschild

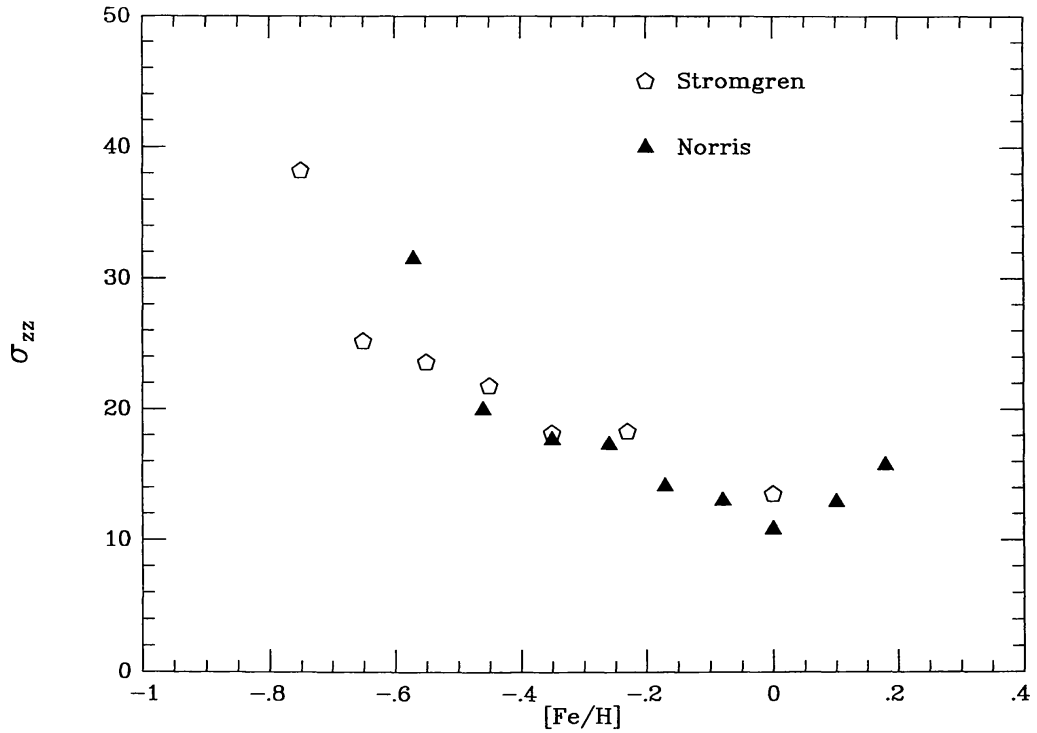

Figure 6b The relationship between [Fe/H] and vertical velocity dispersion for stars near the Sun, from data by Norris (1987c) and Strömgren (1987). These data provide the basis of the arguments that there exists a continuous kinematic relationship between the thick disk and the old disk. One should note particularly the degree of consistency between the data sets and the smoothness or otherwise of the trends at low metallicities, which is where the thick disk first contributes significantly to the data.

1953, Lacey 1984) or spiral density waves (Barbanis & Woltjer 1967, Carlberg & Sellwood 1985), cannot create a population of stars with a scale height such as that inferred for the thick disk, since this is at least an order of magnitude above that of the scatterers themselves, and the heating rate is proportional to the ratio of scale heights (Lacey 1984). A combination of GMCs and spiral density waves can plausibly account for the observed age–velocity dispersion relations for thin disk stars (Binney & Lacey 1988), and since GMCs are observed to occur preferentially in spiral arms, this may be a natural effect (though even this model cannot provide heating beyond $\sigma_z \sim 20$ km s^{-1}). Thus, although the data of Fuchs & Wielen (1987) may be described by known processes, one must appeal to more exotic, high-velocity scatterers to account for any further increase in velocity dispersion. Possibilities include a population of massive black holes (Lacey & Ostriker 1985) or "dark clusters" (Carr & Lacey 1987) in the Galactic halo, and these too have difficulties. The kinematics of thick and thin disks may be similar, but different mechanisms may well be responsible and the similarity misleading.

The rotation velocity of the thick disk is most probably close to that of the old thin disk, lagging behind solar rotation by 30–50 km s^{-1}, as noted above. The earlier determination of a lower rotational velocity, $V_{rot} \sim 100$ km s^{-1} (Wyse & Gilmore 1986), was derived from a proper-motion sample with inherent uncertainties (cf. Norris 1987c). However, as is seen in Figure 3, there do exist well-defined samples of stars with [Fe/H] ~ -0.7 and $V_{rot} \sim 100$ km s^{-1}—in particular, the metal-rich RR Lyrae stars (also of interest for age determinations; see below) and the long-period variables (periods of 150–200 days). Additionally, the spectroscopic survey of Gilmore & Wyse (1987, and in preparation) contains a significant number of stars with these kinematics. As discussed in Section 3.2.2, these stars may provide their own insight into the dynamical history of the Galaxy.

4.3 *Age of the Thick Disk*

An age determination for samples of thick disk stars is an extremely difficult observational problem. In part this is due to the usual difficulty in assigning a reliable age to anything in astronomy, but in this case the situation is complicated by the point noted above that there is no obvious a priori way to define a sample of purely "thick disk" stars. Any sample selected by abundance, kinematics, or chemistry will inevitably include old disk and/or extreme Population II stars in addition to the thick disk. Thus determination of the age of the *youngest* or the *oldest* star in a sample, while tractable, is not an obviously clever way to answer the question of interest. Some information may be derived from Figure 5. It is evident from this figure that the age of the oldest stars with [Fe/H] $\lesssim -0.7$ is comparable to that of the metal-rich globular cluster system, i.e. ~ 14 Gyr (Hesser et al. 1987). This abundance range is expected to be dominated by thick disk stars for $-1 \lesssim$ [Fe/H] $\lesssim -0.8$, which suggests that the most metal-poor thick disk stars are among the oldest in the Galaxy [*modulo* the age determinations of Bell (1988a,b) and Schuster & Nissen (1989) for field subdwarfs of 18 Gyr, which may be interpreted to imply that globular clusters are younger than the field]. More metal-rich thick disk stars may or may not be the same age. It is impossible to determine this from comparison with diagrams like Figure 5, as some old disk stars will contaminate the sample. This point is worth emphasizing, as it removes the rigorous basis for the conclusion of Norris & Green (1989) that the thick disk is several gigayears younger than the disk globular clusters; such a conclusion cannot be derived reliably from photometric data alone. This point is discussed in more detail by Sandage (1988); the interplay between age and metallicity in determining the photometric properties of stellar populations means that one can derive ages from turnoff colors only within the framework of an assumed age-metallicity relationship. The large

intrinsic scatter seen in the age-metallicity relation for local F-dwarfs (Carlberg et al. 1985) and for open clusters (Geisler 1987) will inevitably complicate the determination of the ages of groups of stars from the color of the main-sequence turnoff. Of course, the amplitude of this scatter contains valuable information on the small-scale homogeneity of the interstellar medium in the Galaxy, the history of accretion of satellites (both gaseous and stellar), and the amplitude of large-scale abundance gradients in the Galactic disk.

The morphology of the horizontal branch also in principle contains important information on the age of the thick disk stars, *modulo* the metallicity and the well-known "second parameter" problem. Rose (1985) found a population of red horizontal branch (RHB) candidates with a thick disk configuration and kinematics, which would imply that the thick disk were old if these are truly RHB stars. The thick-disk nature of the kinematics of these stars was confirmed by the high-precision data of Stetson & Aikman (1987), who derived a vertical velocity dispersion of $\sim$45 km s^{-1}. A complication is that Rose found such a large number of candidate RHB stars. In view of the intrinsic rarity of such stars, Rose's result would imply a very large local normalization of the thick disk near the Sun. However, Norris (1987b) and Norris & Green (1989) have argued that these stars are *not* bona fide RHB stars but rather core-helium-burning "clump" stars similar to those seen in open clusters. They argue that their interpretation would mean a higher metallicity for these stars than that of 47 Tuc and hence would lead to a younger age. They infer that the thick disk is at least 3–6 Gyr younger than the disk globular clusters and thus has an age of 8–11 Gyr. However, in addition to the complications with the number of these stars, Janes (1988) has derived an age of 12.5 Gyr for the metal-rich open cluster NGC 6791, which has a well-developed clump, showing explicitly that there is no universal age-metallicity relationship that can be applied.

The *youngest* dated population of RR Lyrae stars is that in the Small Magellanic Cloud cluster NGC 121, which has an age of $\sim$12 Gyr [cf. Olszewski et al. (1987) for a detailed discussion of the age estimates for clump and horizontal branch stars]. The kinematics of the metal-rich RR Lyrae stars ($0 \lesssim \Delta S \lesssim 2$) is that of the thick disk (Sandage 1981, Strugnell et al. 1986), which suggests that 12 Gyr is a lower limit on the age of at least some of the thick disk. Further studies of these metal-rich RR Lyrae stars would be of considerable interest.

Similarly, while the relationship of the globular clusters to field stars is not obvious, *if* the disk globular cluster system studied so well by Zinn (1985) and collaborators [cf. Armandroff (1989) for the most recent analysis] is indeed part of the thick disk, then the antiquity of the thick disk is

reliably established. The rotation velocity of the thick disk globular clusters found by Armandroff (1989) is closer to that of the field thick disk stars than the value derived earlier by Zinn (1985), which could be construed to support the identification of these two populations. However, samples of old disk open clusters *also* have similar kinematics to the field thick disk and hence to the disk globular clusters, which under the same logic would suggest an intimate connection between the open and globular clusters. An understanding of the kinematics of the extant sample of open clusters must take account of the destruction processes that operate preferentially to destroy clusters that are confined to the plane and hence lead to an artificially high scale height and to artificially high velocities for easily observed (i.e. high-latitude) open clusters. The same problem exists for globular clusters, but it will be worse for the more loosely bound open clusters.

All these arguments, however, leave open the possibility of a large age *range* in the thick disk. There is no reliable information yet available on this point; obviously, if one believed *all* of the ages inferred above, then an age spread of several gigayears results. However, this age scatter probably simply reflects the level of uncertainty associated with each of the available age estimates.

5. THE MASS DISTRIBUTION IN THE GALACTIC DISK

The distribution of mass in the Galactic disk is characterized by two numbers: its local *volume* density ρ_0 and its total *surface* density $\Sigma(\infty)$. These are fundamental parameters for many aspects of Galactic structure, such as chemical evolution (is there a significant population of white dwarf remnants from early episodes of massive star formation?), the physics of star formation (how many brown dwarfs are there?), disk galaxy stability (how important dynamically is the self-gravity of the disk?), the properties of dark matter (does the Galaxy contain *dissipational* dark matter, which may then be fundamentally different in nature from the dark matter assumed to provide flat rotation curves?), non-Newtonian gravity theories (where does a description of galaxies with Newtonian gravity and no dark matter fail?), and so on.

Although $\Sigma(\infty)$ and ρ_0 are different measures of the distribution of mass in the Galactic disk near the Sun, they are related. Of the two, the most widely used and commonly determined measure is the local *volume* mass density—i.e. the amount of mass per unit volume near the Sun, which for practical purposes is the same as the volume mass density at the Galactic plane. This quantity has units of $M_\odot$ pc^{-3}, and its local value is often

called the "Oort limit" in honor of the early attempt at its measurement by Oort (1932). The contribution of identified material to the Oort limit may be determined by summing all local observed matter—an observationally difficult task, which leads to considerable uncertainties. These uncertainties arise in part from difficulties in detecting very low-luminosity stars, even very near the Sun (cf. Gilmore et al. 1985, Hawkins & Bessell 1988), in part from uncertainties both in the binary fraction among low-mass stars and in the stellar mass-luminosity relation, but mostly from uncertainties in determining the volume density of the ISM. This latter uncertainty is exacerbated by the fact that the physically important quantity (for dynamical purposes) is the mean volume density of the patchily distributed ISM at the solar Galactocentric distance. The best available determination of the local mass density in identified material is $\sim 0.1\ M_\odot$ pc^{-3}.

The second measure of the distribution of mass in the solar vicinity is the integral surface mass density. This quantity has units of $M_\odot\ \mathrm{pc}^{-2}$ and is the total amount of disk mass in a column perpendicular to the Galactic plane. It is this quantity that is required for the deconvolution of rotation curves into disk, bulge, and dark halo contributions to the large-scale distribution of mass in galaxies. The most recent determination of this surface mass density, prior to that discussed below, is by Bahcall (1984a), who derives values in the range 55–80 $M_\odot\ \mathrm{pc}^{-2}$. As an indication of the dynamical significance of this mass density, the contribution of a disk potential generated by this local mass density to the local circular velocity, if we assume an exponential disk with the Sun 2.5 radial scale lengths from the Galactic center, is

$$V_{\mathrm{circ,\,disk}} \sim 150\left(\frac{\Sigma_{\mathrm{local}}}{60\ M_\odot\ \mathrm{pc}^{-2}}\right)^{1/2}\ \mathrm{km\ s}^{-1}. \qquad 17.$$

The local circular velocity is $\sim 220\ \mathrm{km\ s}^{-1}$, and the contributions to this circular velocity from the various components generating the Galactic potential add in quadrature. Thus, the Galactic disk is far from dominating the local potential well.

Both these dynamical quantities are derived from a measurement of the vertical Galactic force field $K_z(z)$. If one knew both the local *volume* mass density and the integral *surface* mass density of the Galactic disk, one could immediately constrain the scale height of any contribution to the local volume mass density that was not identified. For example, one might suspect that some fraction of the local volume mass density was unidentified (i.e. a local "missing-mass" problem) but also determine a surface density that is effectively fully explained by observed mass. Then the

unidentified contribution to the local volume density would have to have a small scale height in order that its contribution to the surface density be small. In view of the very small scale length on which it must be distributed, it would then be plausible to deduce that any local "missing" mass unidentified in the volume mass density near the Sun was not the "missing" mass that dominates the extended outer parts of galaxies.

Determination of the volume mass density and the integral surface mass density near the Sun requires similar observational data—namely, distances and velocities for a suitable sample of tracer stars—but rather different analyses.

5.1 *Measurement of the Galactic Potential*

All determinations of the mass distribution in the Galactic disk require a solution of the collisionless Boltzmann equation. In view of its intractability, in practice one utilizes its vertical moment, the vertical Jeans' equation (Equation 10), which we repeat here for convenience:

$$K_z = \frac{1}{\nu}\frac{\partial}{\partial z}(\nu\sigma_{zz}) + \frac{1}{r\nu}\frac{\partial}{\partial r}(r\nu\sigma_{rz}), \qquad 18.$$

where $\nu(r, z)$ is the space density of the stars, and $\sigma_{ij}(r, z)$ is their velocity dispersion tensor.

The first term on the right-hand side of this equation is dominant and contains a logarithmic derivative of the stellar space density $\nu(r, z)$ and a derivative of the vertical velocity dispersion, σ_{zz}. Since the stellar population in the solar neighborhood is, within a multiplicative factor of a few, tolerably well described by an isothermal stellar population, the term containing the derivative of the space density dominates the determination of $K_z(z)$ near the Sun. This point is not often appreciated adequately, but it means that one should determine stellar density profiles with even greater care than that required for the velocity dispersions.

The second term in the Jeans' equation describes the tilt of the stellar velocity ellipsoid away from the local cylindrical-polar coordinate system in which velocity dispersions are measured. One therefore needs the r-gradients of σ_{rz} and of ν. There are no general analytical solutions for this term, but one may derive a realistic upper limit on its importance by considering velocity ellipsoids that are oriented toward the Galactic center. In this case, if the disk of the Galaxy is self-gravitating, radially exponential, and has a constant vertical scale height, as is seen in external disk galaxies, vertical balance implies (for disk surface density μ) that $\sigma_{zz} \propto \mu$, and hence that

$$\sigma_{zz} \propto \mu \propto \nu \propto e^{-r/h_r}. \qquad 19.$$

Thus we obtain

$$\frac{1}{rv}\frac{\partial}{\partial r}(rv\sigma_{rz}) = 2(\alpha^2-1)\sigma_{zz}\left[\frac{\alpha^2 z^3}{(\alpha^2 z^2+r^2)^2} - \frac{rz}{h_r(\alpha^2 z^2+r^2)}\right] \quad 20.$$

as the tilting term for a radially exponential population of constant vertical scale height with a velocity ellipsoid of constant axis ratio α that points at the Galactic center (Kuijken & Gilmore 1989a). Since this term is proportional to σ_{zz}, inserting it into the Jeans' equation (Equation 18) gives a linear equation in σ_{zz}, from which one can deduce K_z.

Given a measurement of the gravitational field $\mathbf{K}(r, z)$ in an axisymmetric galaxy, the total density ρ of gravitating matter follows from Poisson's equation:

$$\nabla\cdot\mathbf{K} = -4\pi G\rho. \quad 21.$$

In the case of a disk galaxy, we can express the r-gradient in $\nabla\cdot\mathbf{K}$ in terms of the observed circular velocity at the Sun, v_c, or in terms of the Oort constants of Galactic rotation, A and B (see, for example, Mihalas & Binney 1981):

$$\begin{aligned}\rho &= -\frac{1}{4\pi G}\left[\frac{\partial K_z}{\partial z} + \frac{1}{r}\frac{\partial}{\partial r}(rK_r)\right] \\ &= -\frac{1}{4\pi G}\left[\frac{\partial K_z}{\partial z} + \frac{1}{r}\frac{\partial(v_c^2)}{\partial r}\right] \\ &= -\frac{1}{4\pi G}\left[\frac{\partial K_z}{\partial z} + 2(A^2-B^2)\right]. \quad 22.\end{aligned}$$

For a disk galaxy with an approximately flat rotation curve the second term is small within a few kiloparsecs of the disk plane (for an exactly flat rotation curve, we have $A^2-B^2 \equiv 0$ at $z = 0$; Kuijken & Gilmore 1989a), so we can integrate in z to obtain the total column density $\Sigma(z)$ between heights $-z$ and z relative to the disk plane $z = 0$:

$$\Sigma(z) = \int_{-|z|}^{|z|}\rho(z)\,dz = \frac{|K_z|}{2\pi G} - \frac{(A^2-B^2)}{\pi G}|z|. \quad 23.$$

It is evident from the equations above that determinations of the local volume mass density ρ_0 depend on the square of any distance scale errors in the tracer population, since they are derived from the second derivative of the stellar space density distribution, while determinations of the surface mass density are linearly proportional to the distance scale, being based on the first derivative.

Recently, Bahcall (1984a,b,c) has improved the theoretical methods

with which to determine the local volume density of matter, ρ_0. He has reanalyzed the available F-dwarf and K-giant high-Galactic-latitude data with new, self-consistent Galaxy models (in the sense that the matter that generates the gravitational field itself responds to it via the collisionless Boltzmann equation and including a dark halo needed to support a flat rotation curve) to replace the simpler models that had been used up to that time. He found that (*a*) the gravitational field due to the 0.10 $M_\odot$ pc^{-3} of stars and gas that are identified in the solar neighborhood is inconsistent with the gravitational field derived from the data; and (*b*) depending on its scale height, a further 0.06–0.14 $M_\odot$ pc^{-3} of unidentified matter is required. This matter is not part of a spherical halo: The local volume density required in the dark halo to explain the rotation curve is only ~ 0.01 $M_\odot$ pc^{-3}, with this value being insensitive to the local disk mass. Hence, this result implies significant amounts of disklike, dissipational dark matter in the solar neighborhood.

The analytical techniques developed by Bahcall (1984a,b,c) represent a considerable improvement over those applied previously and for the first time allow a derivation of ρ_0 that is limited by the quality of the available observational data rather than by the approximate nature of the analysis. Bahcall's analysis is primarily appropriate for determination of ρ_0 and is less suitable for the determination of $\Sigma(\infty)$. Kuijken & Gilmore (1989a,b) therefore developed a new technique for the analysis of stellar kinematic data, which is more appropriate for determination of the integral surface mass density of the Galactic disk near the Sun. Their analysis involves maximum-likelihood comparison of observed and predicted *distribution functions* of stellar velocities as a function of distance from the plane. It thus removes the need to describe an array of distance-velocity data by moments, such as the rms velocity dispersion. It also provides the freedom to include important physical effects (the orientation of the stellar velocity ellipsoid far from the Galactic plane) and constraints (consistency with the Galactic rotation curve) in the modeling.

The study by Kuijken & Gilmore (1989a,b) utilized a new set of data for K-dwarf stars extending to 2 kpc from the disk plane. From these data, they measure a total disk surface mass density of $\Sigma(\infty) = 46 \pm 9$ $M_\odot$ pc^{-2}. The corresponding identified surface mass density, deduced by integrating local stellar data through their derived $K_z(z)$ law and adding the directly observed mass in the interstellar medium, is 48 ± 8 $M_\odot$ pc^{-2}. [The errors on this latter value arise from uncertainties in the mean value of the molecular gas density appropriate at the solar Galactocentric distance, and in the density of stars near the plane, where area-limited star count surveys are insensitive. The errors on the former value have been estimated as ± 12 $M_\odot$ pc^{-2} from analyses of simulated data by Gould (1989) and

Statler (1989).] Thus the 1σ *upper bound* on the surface density of any unidentified matter in the solar neighborhood is about 10 $M_\odot$ pc^{-2}, while the most likely value is no unidentified mass at all.

5.2 *Determination of the Local Volume Mass Density*

Determination of the local *volume* mass density near the Sun—the Oort limit—typically shows that perhaps 50% of the mass measured dynamically remains unidentified. Measurement of the *surface* mass density of the Galactic disk near the Sun shows no significant difference between the disk mass measured dynamically and the identified disk mass. Thus, either the unidentified mass in the Oort limit has a very small scale height, so that the *total* amount of dark mass remains insignificantly small—in effect, it must be distributed like the cold interstellar medium—or systematic errors remain in the determination of the Oort limit [cf. Kuijken & Gilmore (1989c) for details].

The specific limit derived to allow consistency between detection of significant unidentified mass in the local volume and no detection of significant unidentified mass in the local column, is that any local dark matter with volume density ρ_0 must be distributed with an effective scale height of $2H$ [such that $\Sigma = 2\rho_0 H$], where

$$\rho_{\text{unident}} < \frac{10\ M_\odot\ \text{pc}^{-2}}{2H}. \qquad 24.$$

Large amounts of missing matter in the volume density require a small scale height to be consistent with the measurement of $\Sigma(\infty)$. For example, if one really believed that 0.085 $M_\odot$ pc^{-3} were unidentified in the local volume mass density, then this unidentified mass must be distributed with a scale height of $\lesssim 60$ pc.

In view of this rather severe scale height limitation, it is of interest to reexamine the uncertainties in the determination of the Oort limit. The sensitivity of determinations of the local volume mass density ρ_0 to uncertain data lies in the modeling of the stellar velocity distribution near the Galactic plane and in the determination of the stellar density distribution with distance from this plane. Both F-dwarf and K-giant tracer samples have been analyzed to determine ρ_0, with both producing a result of $\rho_0 \sim 0.20\ M_\odot$ pc^{-3}, where the identified mass provides $\rho_{0,\text{obs}} = 0.10\ M_\odot$ pc^{-3} (Bahcall 1984c).

The effect of *random* errors on determinations of the Oort limit has been discussed in detail by Gilden & Bahcall (1985), who conclude that these errors produce an unbiased uncertainty of $\sim 12\%$, and by Bienaymé et al. (1987) and Crézé et al. (1989), who conclude that random errors produce

an uncertainty of $\sim 50\%$ and also produce a bias toward an erroneous detection of unidentified mass. The difference in these results is due to different techniques for handling observational errors in the simulations, which suggests that the appropriate uncertainty to apply to determinations of the Oort limit is substantially larger than that due to Poisson statistical noise. Potentially large *systematic* problems with the data remain and have been discussed by Kuijken & Gilmore (1989c).

The F-star sample analyzed is the sum of two subsamples (F5 and F8; Hill et al. 1979), with no evidence for a difference between their velocity distributions (Adamson et al. 1988). For steady-state stellar populations, two tracer populations with the same kinematics in the same gravitational potential must follow the same spatial density distribution. For the F5 and F8 samples this is not the case (Figure 7*a*). One or both of the data and the assumptions underlying the modeling of the F-star kinematics are thus clearly in error. The amplitude of the resulting uncertainty can be found by deducing ρ_0 from each of the three F-star samples (F5, F5+F8, and F8) by using the algorithm derived by Bahcall (1984a). The resulting values of ρ_0 are 0.29 $M_\odot$ pc^{-3}, 0.185 $M_\odot$ pc^{-3} [reproducing the result derived by

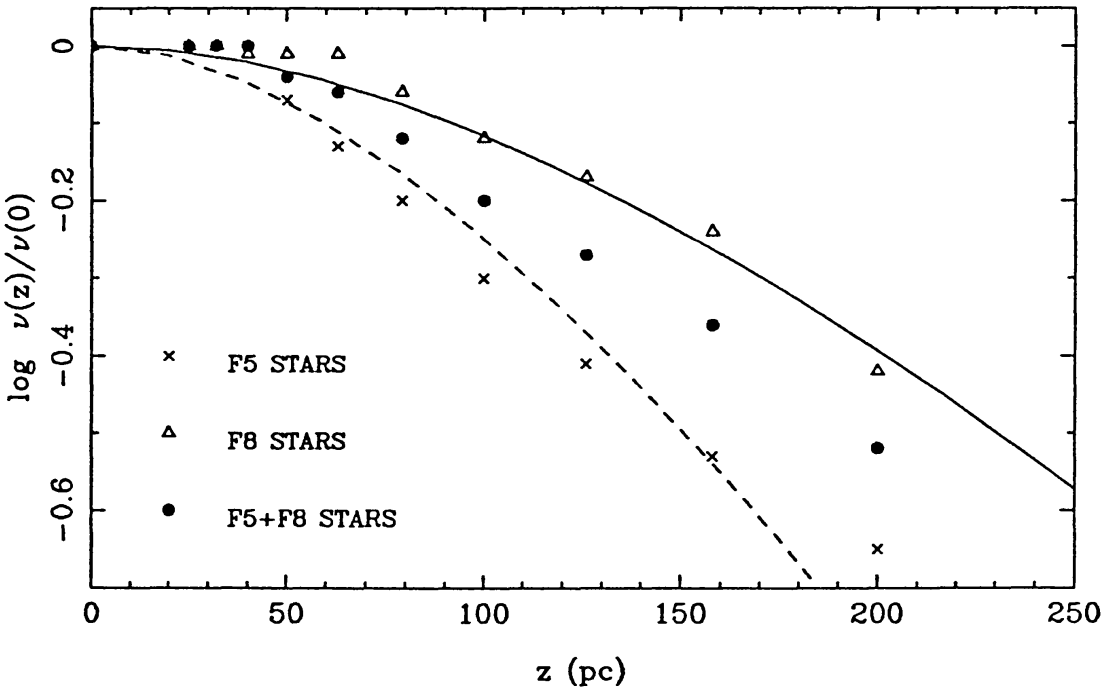

Figure 7a The Hill et al. (1979) F-star samples. The difference between the density profiles of the F5 and the F8 samples is evident. The curves show separate model fits calculated using the algorithm devised by Bahcall (1984a) to the F5 and the F8 subsets of the data defined by Hill et al. Only the averaged sample (solid dots) was analyzed by Bahcall (1984b). The models shown have local volume mass densities $\rho_0 = 0.11\ M_\odot$ pc^{-3} [i.e. with no missing mass (solid line)] and $\rho_0 = 0.29\ M_\odot$ pc^{-3} (dashed line).

Bahcall (1984b) exactly], and 0.11 $M_\odot$ pc^{-3}, respectively. Thus one may deduce that there is twice as much mass missing as observed in the local volume density, just as much mass missing as observed, or no missing mass at all, depending on which sample of stars one chooses to analyze. Clearly, the available F-star data are not capable of providing any evidence either for or against the concept of missing mass near the Sun.

The sample of K giants, which has been analyzed previously, has been shown to have a velocity distribution that is consistent with a single isothermal, with a velocity dispersion of $\sim$20 km s^{-1} (Bahcall 1984c). Thus, unlike the F stars, in this model the K-giants consist entirely of old disk stars, with neither young disk nor thick disk star representatives. Since stars of a wide range of masses become K-giants, including the present F-dwarfs, this model is inherently implausible. Consistency with an isothermal is presumably an artifact of small number statistics near the Galactic plane, where lower velocity dispersion samples would be found. The K-giant density law is also uncertain, as the relevant color-magnitude relation is a strong function of age and metallicity, both of which appear to be correlated with distance from the Galactic plane. Higher precision data than those published to date are necessary to derive a reliable density profile.

A further complication follows from a feature of previous analyses, which assign high weight to the density profile near the plane (where the number of stars counted is smallest). Reanalysis of published data, including weighting of the density data by its Poisson noise and using a more detailed fit to the local velocity data from Hill (1960), leads to a value of $\rho_0 = 0.10\ M_\odot$ pc^{-3}, that is, *no* missing mass (Figure 7*b*; cf. Kuijken & Gilmore 1989c). The previously derived value from the same data using the same analysis technique was $\rho_0 = 0.21\ M_\odot$ pc^{-3}, that is, 50% missing mass (Bahcall 1984c).

We conclude that available determinations of the volume mass density near the Sun—the Oort limit—remain limited by systematic and random difficulties with the available data. One may deduce a local unexplained mass density that is up to a factor of two larger than the mass density that is identified with stars and the interstellar medium near the Sun from some samples of (young) F-stars. Other samples of (older) F-stars and of K-giants, when analyzed using velocity distributions consistent with the structure of the local Galactic disk, provide no evidence for any unexplained mass near the Sun. Determinations of the integral *surface* mass density of the Galactic disk near the Sun also show evidence for no missing mass in the Galactic disk. In brief, available data either are internally inconsistent or provide no robust evidence for the existence of any missing mass associated with the Galactic disk.

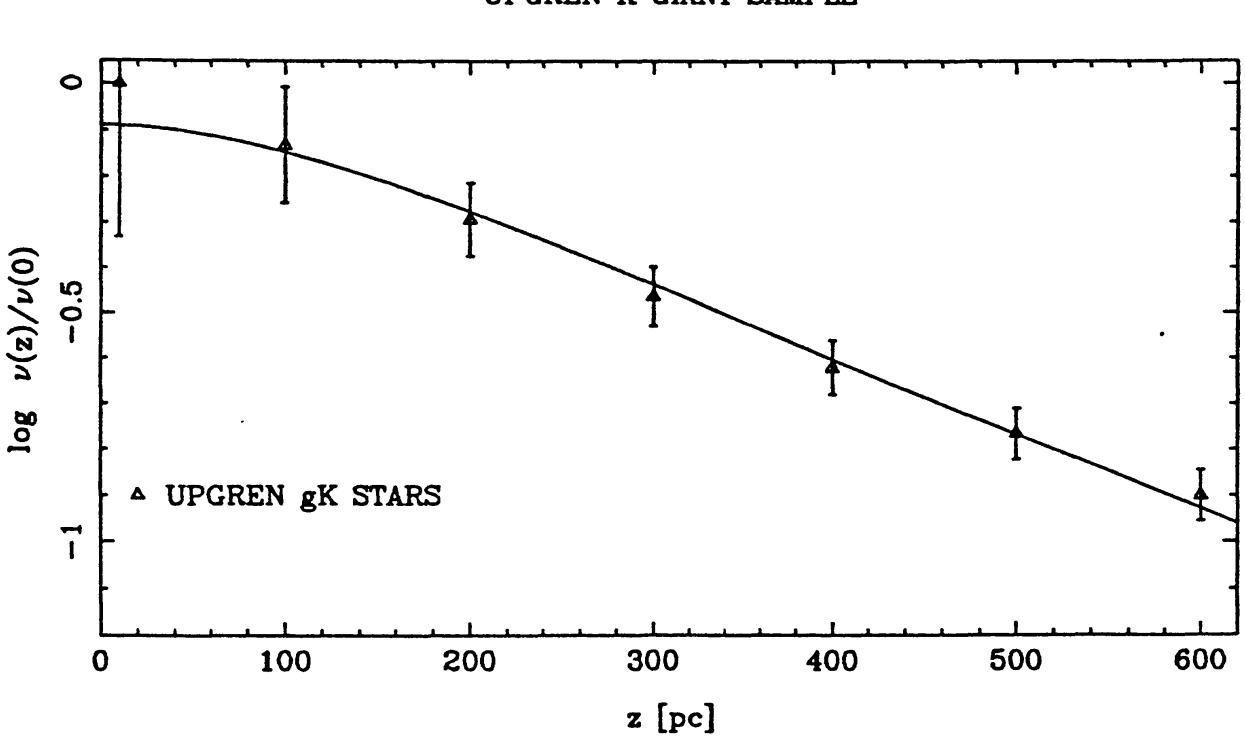

Figure 7b Weighted fit to the Upgren (1962) K-giant density distribution, using the velocity distribution measured by Hill (1960). The model shown contains no dark matter in the Galactic disk and has $\rho_0 = 0.10\ M_\odot\ \mathrm{pc}^{-3}$.

This result has many important implications, some of which are discussed by Kuijken & Gilmore (1989b). It confirms that at least in our Galaxy, a "maximal disk" fit to explain extended flat rotation curves is not viable. It disproves available models of chemical (and luminosity) evolution that require preferential formation of high-mass stars (e.g. by a bimodal stellar initial mass function) in the early evolution of the Galactic disk. Extrapolations of the stellar initial mass function that result in significant mass in substellar mass "brown dwarfs" are ruled out. It implies that the disk is comfortably stable against axisymmetric local perturbations (the Toomre Q parameter for the stellar disk has a local value of ~ 2.1, where $Q > 1$ implies stability, though the destabilizing effect of the relatively large mass of cold gas should probably not be neglected) and just stable against global bar-mode instabilities. Severe constraints can be set on most available alternative theories to Newtonian gravity, with the local gravitational potential gradient deduced from recent K-dwarf data being inconsistent with the most recently suggested modifications to the theory of gravity.

ACKNOWLEDGMENTS

GG and RFGW are grateful to the NATO Scientific Affairs Division for a travel grant to aid their collaboration. RFGW acknowledges partial support from the National Science Foundation (grant AST-88-07799) and thanks the UC Berkeley Astronomy Department and CITA for hospitality during the writing of some of this paper. We thank the many colleagues who facilitated the writing of this review by providing results and papers in advance of publication.

Literature Cited

Adamson, A. J., Hill, G., Fisher, W., Hilditch, R. W., Sinclair, C. D. 1988. *MNRAS* 230: 273
Armandroff, T. 1989. *Astron. J.* 97: 375
Arnett, W. D. 1978. *Ap. J.* 219: 1008
Bahcall, J. N. 1984a. *Ap. J.* 276: 156
Bahcall, J. N. 1984b. *Ap. J.* 276: 169
Bahcall, J. N. 1984c. *Ap. J.* 287: 926
Bahcall, J. N. 1986. *Annu. Rev. Astron. Astrophys.* 24: 577
Bahcall, J. N., Ratnatunga, K. U., Buser, R., Fenkart, R. P., Spaenhauer, A. 1985. *Ap. J.* 299: 616
Bahcall, J. N., Soneira, R. M. 1980. *Ap. J. Suppl.* 44: 73 (BS)
Bahcall, J. N., Soneira, R. M. 1981. *Ap. J. Suppl.* 47: 357
Bahcall, J. N., Soneira, R. M. 1984. *Ap. J. Suppl.* 55: 67 (BS)
Barbanis, B., Woltjer, L. 1967. *Ap. J.* 150: 461
Barnes, J., Efstathiou, G. 1987. *Ap. J.* 319: 575
Bell, R. A. 1988a. *Astron. J.* 95: 1484
Bell, R. A. 1988b. In *The Calibration of Stellar Ages*, ed. A. G. D. Philip, p. 163. Schenectady, NY: L. Davis Press
Bienaymé, O., Robin, A., Crézé, M. 1987. *Astron. Astrophys.* 180: 94
Binney, J. 1977. *Ap. J.* 215: 483
Binney, J., Lacey, C. G. 1988. *MNRAS* 230: 597
Binney, J., May, A. 1986. *MNRAS* 218: 743
Blanco, V. M., Blanco, B. M. 1986. *Astrophys. Space Sci.* 118: 365
Blauuw, A., Schmidt, M., eds. 1965. *Galactic Structure* (*Stars and Stellar Systems*, Vol. 5). Chicago: Univ. Chicago Press
Blumenthal, G. R., Faber, S. M., Primack, J. R., Rees, M. J. 1984. *Nature* 311: 517
Bok, B. J., Basinski, J. 1962. *Mem. Mt. Stromlo Obs.* 4: 1
Bok, B. J., MacRae, D. A. 1942. *Ann. NY Acad. Sci.* 42: 219
Bothun, G. D., Impey, C. D., Malin, D. F., Mould, J. R. 1987. *Astron. J.* 94: 23
Brooks, K. 1981. PhD thesis. Univ. Calif., Berkeley
Buser, R. 1988. In *Impacts des Surveys du Visible Sur Notre Connaisance de la Galaxie. C. R. Journ. Strasbourg*, p. 115
Buser, R., Kaeser, U. 1985. *Astron. Astrophys.* 145: 1
Carlberg, R. G. 1985. In *The Milky Way Galaxy*, *IAU Symp. No. 106*, ed. H. van Woerden, W. B. Burton, R. J. Allen, p. 615. Dordrecht: Reidel
Carlberg, R. G., Dawson, P., Hsu, T., Vanden Berg, D. A. 1985. *Ap. J.* 294: 674
Carlberg, R. G., Sellwood, J. A. 1985. *Ap. J.* 292: 79
Carney, B., Aguilar, L., Latham, D. W., Laird, J. B. 1989b. Submitted for publication
Carney, B., Latham, D. W. 1986. *Astron. J.* 92: 60
Carney, B., Latham, D. W., Laird, J. B. 1989a. *Astron. J.* 97: 423
Carr, B. J., Lacey, C. G. 1987. *Ap. J.* 316: 23
Chiu, L.-T. G. 1980. *Ap. J. Suppl.* 44: 31
Conlon, E. S., Brown, P. J. F., Dufton, P. L., Keenan, F. P. 1988. *Astron. Astrophys.* 200: 168
Crézé, M., Robin, A., Bienaymé, O. 1989. *Astron. Astrophys.* 211: 1
Dejonghe, H., de Zeeuw, P. T. 1988. *Ap. J.* 329: 720
del Rio, G., Fenkart, R. 1987. *Astron. Astrophys. Suppl.* 68: 397
Disney, M. 1976. *Nature* 263: 573
Eggen, O. J. 1979. *Ap. J.* 229: 158
Eggen, O. J. 1987. In *The Galaxy*, ed. G. Gilmore, B. Carswell, p. 211. Dordrecht: Reidel
Eggen, O. J., Lynden-Bell, D., Sandage, A. 1962. *Ap. J.* 136: 748 (ELS)
Elvius, T. 1965. See Blaauw & Schmidt 1965, Chap. 3
Evans, D. W. 1987. *MNRAS* 227: 13P
Fall, S. M. 1987. In *Towards Understanding*

Galaxies at High Redshift, ed. R. Kron, A. Renzini, p. 15. Dordrecht: Reidel
Fall, S. M., Efstathiou, G. 1980. *MNRAS* 193: 189
Fall, S. M., Rees, M. J. 1977. *MNRAS* 181: 37P
Fall, S. M., Rees, M. J. 1985. *Ap. J.* 298: 18
Feast, M. 1987. In *The Galaxy*, ed. G. Gilmore, B. Carswell, p. 1. Dordrecht: Reidel
Fenkart, R. P. 1989. *Astron. Astrophys. Suppl.* In press
Freeman, K. C. 1987. *Annu. Rev. Astron. Astrophys.* 25: 603
Frenk, C. S., White, S. D. M. 1980. *MNRAS* 193: 295
Frenk, C. S., White, S. D. M., Davis, M., Efstathiou, G. 1988. *Ap. J.* 327: 507
Frenk, C. S., White, S. D. M., Efstathiou, G., Davis, M. 1985. *Nature* 317: 595
Friel, E. D. 1987. *Astron. J.* 93: 1388
Friel, E. D. 1988. *Astron. J.* 95: 1727
Friel, E. D., Cudworth, K. M. 1986. *Astron. J.* 91: 293
Frogel, J. A. 1988. *Annu. Rev. Astron. Astrophys.* 26: 51
Fuchs, B., Wielen, R. 1987. In *The Galaxy*, ed. G. Gilmore, B. Carswell, p. 375. Dordrecht: Reidel
Gallagher, J. S., Hunter, D. A., Tutukov, A. V. 1984. *Ap. J.* 284: 544
Geisler, G. 1987. *Astron. J.* 94: 84
Gilden, D. L., Bahcall, J. N. 1985. *Ap. J.* 296: 240
Gilmore, G. 1981. *MNRAS* 195: 183
Gilmore, G. 1983. In *Nearby Stars and the Stellar Luminosity Function*, ed. A. G. D. Philip, A. R. Upgren, pp. 197, 221. Schenectady, NY: L. Davis Press
Gilmore, G. 1984a. In *Astronomy With Schmidt-Type Telescopes*, ed. M. Capaccioli, p. 77. Dordrecht: Reidel
Gilmore, G. 1984b. *MNRAS* 207: 223
Gilmore, G., Hewett, P. C. 1983. *Nature* 306: 669
Gilmore, G., Hewett, P. C. 1989. In preparation
Gilmore, G., Reid, I. N. 1983. *MNRAS* 202: 1025
Gilmore, G., Reid, I. N., Hewett, P. C. 1985. *MNRAS* 213: 257
Gilmore, G., Wyse, R. F. G. 1985. *Astron. J.* 90: 2015
Gilmore, G., Wyse, R. F. G. 1986. *Nature* 322: 806
Gilmore, G., Wyse, R. F. G. 1987. In *The Galaxy*, ed. G. Gilmore, B. Carswell, p. 247. Dordrecht: Reidel
Gilroy, K. K., Sneden, C., Pilachowski, C., Cowan, J. J. 1988. *Ap. J.* 327: 298
Gould, A. 1989. *Ap. J.* In press
Gunn, J. E. 1982. In *Astrophysical Cosmology*, ed. H. A. Brück, G. V. Coyne, M. S. Longair, p. 233. Vatican City: Pontif. Acad. Sci.
Gunn, J. E., Gott, J. R. 1972. *Ap. J.* 176: 1
Habing, H. J. 1987. In *The Galaxy*, ed. G. Gilmore, B. Carswell, p. 173. Dordrecht: Reidel
Harmon, R. T., Gilmore, G. 1988. *MNRAS* 235: 1025
Harris, W. 1981. *Astron. J.* 86: 719
Hartkopf, W. I., Yoss, K. M. 1982. *Astron. J.* 87: 1679
Hartwick, F. D. A. 1976. *Ap. J.* 209: 418
Hartwick, F. D. A. 1987. In *The Galaxy*, ed. G. Gilmore, B. Carswell, p. 281. Dordrecht: Reidel
Hawkins, M. R. S., Bessell, M. 1988. *MNRAS* 234: 177
Hernquist, L., Quinn, P. J. 1989. Submitted for publication
Hesser, J. E., Harris, W. E., Vanden Berg, D. A., Allwright, J. W. B., Shott, P., Stetson, P. B. 1987. *Publ. Astron. Soc. Pac.* 99: 739
Hill, E. R. 1960. *Bull. Astron. Inst. Neth.* 15: 1
Hill, G., Hilditch, R. W., Barnes, J. V. 1979. *MNRAS* 186: 813
Iben, I. 1985. In *Nucleosynthesis*, ed. W. D. Arnett, J. W. Truran, p. 272. Chicago: Univ. Chicago Press
Iben, I. 1986. In *Cosmogonical Processes*, ed. W. D. Arnett, C. J. Hansen, J. W. Truran, S. Tsuruta, p. 155. Utrecht: VNU Sci. Press
Isobe, S. 1974. *Astron. Astrophys.* 36: 333
Janes, K. 1988. In *The Calibration of Stellar Ages*, ed. A. G. D. Philip, p. 59. Schenectady, NY: L. Davis Press
Jones, B. J. T., Wyse, R. F. G. 1983. *Astron. Astrophys.* 120: 165
Keenan, F. P., Lennon, D. J., Brown, P. J. F., Dufton, P. L. 1986. *Ap. J.* 307: 694
King, I. R. 1986. In *Stellar Populations*, ed. C. Norman, A. Renzini, M. Tosi, p. 238. Cambridge: Univ. Press
Kinman, T. D., Wirtanen, C. A., Janes, K. A. 1966. *Ap. J. Suppl.* 13: 379
Klemola, A. R., Jones, B. F., Hanson, R. B. 1987. *Astron. J.* 94: 501
Knude, J., Schnedler Nielsen, H., Winther, M. 1987. *Astron. Astrophys.* 179: 115
Koo, D. C., Kron, R. G. 1982. *Astron. Astrophys.* 105: 107
Koo, D. C., Kron, R. G., Cudworth, K. 1986. *Publ. Astron. Soc. Pac.* 98: 285
Kraft, R. 1988. In *New Ideas in Astronomy*, ed. F. Bertola, J. W. Sulentic, B. F. Madore, p. 23. Cambridge: Univ. Press
Kron, R. G. 1980. *Ap. J. Suppl.* 43: 305
Kuijken, K., Gilmore, G. 1989a. *MNRAS.* In press (Pap. I)
Kuijken, K., Gilmore, G. 1989b. *MNRAS.* In press (Pap. II)

Kuijken, K., Gilmore, G. 1989c. *MNRAS*. In press (Pap. III)
Lacey, C. G. 1984. *MNRAS* 208: 687
Lacey, C. G., Ostriker, J. P. 1985. *Ap. J.* 299: 633
Laird, J. B., Carney, B. W., Latham, D. W. 1988a. *Astron. J.* 95: 1843
Laird, J. B., Rupen, M. P., Carney, B. W., Latham, D. W. 1988b. *Astron. J.* 96: 1908
Lance, C. M. 1988. *Ap. J.* 334: 927
Larson, R. B. 1976. *MNRAS* 176: 31
Larson, R. B., Tinsley, B. M., Caldwell, C. N. 1980. *Ap. J.* 237: 692
Levison, H. F., Richstone, D. O. 1986. *Ap. J.* 308: 627
Lewis, J., Freeman, K. C. 1989. *Astron. J.* 97: 139
Lynden-Bell, D. 1967a. *MNRAS* 136: 101
Lynden-Bell, D. 1967b. In *Radio Astronomy and the Galactic System, IAU Symp. No. 31*, ed. H. van Woerden, p. 257. London: Academic
Matteucci, F., Greggio, L. 1986. *Astron. Astrophys.* 154: 279
May, A., van Albada, T. J. 1984. *MNRAS* 209: 15
McGlynn, T. 1984. *Ap. J.* 281: 13
McNeil, R. C. 1986. *Astron. J.* 92: 335
Mihalas, D., Binney, J. 1981. *Galactic Astronomy*. San Francisco: Freeman
Miller, G. E., Scalo, J. M. 1979. *Ap. J. Suppl.* 41: 513
Morrison, H. L., Flynn, C., Freeman, K. C. 1989. Submitted for publication
Norris, J. 1986. *Ap. J. Suppl.* 61: 667
Norris, J. 1987a. In *The Galaxy*, ed. G. Gilmore, B. Carswell, p. 297. Dordrecht: Reidel
Norris, J. 1987b. *Astron. J.* 93: 616
Norris, J. 1987c. *Ap. J. Lett.* 314: L39
Norris, J., Bessell, M. S., Pickles, A. J. 1985. *Ap. J. Suppl.* 58: 463
Norris, J., Green, E. M. 1989. *Ap. J.* 337: 272
Norris, J., Ryan, S. G. 1989a. *Ap. J. Lett.* 336: L17
Norris, J., Ryan, S. G. 1989b. *Ap. J.* 340: 739
O'Connell, D. J. K., ed. 1958. *Stellar Populations*. Amsterdam: North-Holland
Olszewski, E. W., Schommer, R. A., Aaronson, M. 1987. *Astron. J.* 93: 565
Oort, J. H. 1932. *Bull. Astron. Inst. Neth.* 6: 249
Oort, J. H. 1958. See O'Connell 1958, p. 415
Oort, J. H. 1965. See Blaauw & Schmidt 1965, Chap. 21
Oort, J. H., Plaut, L. 1975. *Astron. Astrophys.* 41: 71
Osvalds, V., Risley, A. M. 1961. *Publ. Leander McCormick Obs.*, Vol. 11, Part 21
Pagel, B. E. J., Patchett, B. E. 1975. *MNRAS* 172: 13
Plaut, L. 1965. See Blaauw & Schmidt 1965, Chap. 13
Pritchet, C. 1983. *Astron. J.* 88: 1476
Ratnatunga, K. U., Bahcall, J. N., Casertano, S. 1989. *Ap. J.* 339: 106
Ratnatunga, K. U., Freeman, K. C. 1985. *Ap. J.* 291: 260
Ratnatunga, K. U., Freeman, K. C. 1989. *Ap. J.* 339: 126
Rees, M. J., Ostriker, J. P. 1977. *MNRAS* 179: 541
Reid, I. N., Gilmore, G. 1982. *MNRAS* 201: 73
Robin, A., Crézé, M. 1986a. *Astron. Astrophys. Suppl.* 64: 53
Robin, A., Crézé, M. 1986b. *Astron. Astrophys.* 157: 71
Rodgers, A., Harding, P. 1989. *Astron. J.* 97: 1036
Rodgers, A., Harding, P., Ryan, S. 1986. *Astron. J.* 92: 600
Rodgers, A. W., Paltoglou, G. 1984. *Ap. J. Lett.* 283: L5
Rose, J. 1985. *Astron. J.* 90: 803
Ryden, B. S. 1988. *Ap. J.* 329: 589
Sandage, A. 1981. *Astron. J.* 86: 1643
Sandage, A. 1987a. In *The Galaxy*, ed. G. Gilmore, B. Carswell, p. 321. Dordrecht: Reidel
Sandage, A. 1987b. *Astron. J.* 93: 610
Sandage, A. 1988. In *The Calibration of Stellar Ages*, ed. A. G. D. Philip, p. 43. Schenectady, NY: L. Davis Press
Sandage, A., Fouts, G. 1987. *Astron. J.* 92: 74
Schombert, J. M., Bothun, G. 1987. *Astron. J.* 93: 60
Schuster, W., Nissen, P. 1989. *Astron. Astrophys.* In press
Searle, L. 1977. In *The Evolution of Galaxies and Stellar Populations*, ed. B. M. Tinsley, R. B. Larson, p. 219. New Haven, Conn: Yale Univ. Press
Searle, L., Zinn, R. 1978. *Ap. J.* 225: 357
Shaw, M., Gilmore, G. 1989. *MNRAS* 237: 903
Silk, J. 1977. *Ap. J.* 211: 638
Silk, J. 1983. *Nature* 301: 574
Sommer-Larsen, J. 1987. *MNRAS* 227: 21P
Sommer-Larsen, J., Christensen, P. R. 1987. *MNRAS* 225: 499
Sommer-Larsen, J., Christensen, P. R. 1989. Preprint
Spitzer, L., Schwarzschild, M. 1953. *Ap. J.* 118: 106
Statler, T. S. 1988. *Ap. J.* 331: 71
Statler, T. S. 1989. *Ap. J.* In press
Stetson, P. B., Aikman, G. C. L. 1987. *Astron. J.* 93: 1439
Stetson, P. B., Harris, W. E. 1988. *Astron. J.* 96: 909

Stobie, R. S., Ishida, K. 1987. *Astron. J.* 93: 624
Strömgren, B. 1987. In *The Galaxy*, ed. G. Gilmore, B. Carswell, p. 229. Dordrecht: Reidel
Strugnell, P., Reid, I. N., Murray, C. A. 1986. *MNRAS* 220: 413
Tammann, G. 1982. In *Supernovae: A Survey of Current Research*, ed. M. J. Rees, R. J. Stoneham, p. 371. Cambridge: Univ. Press
Terndrup, D. M. 1988. *Astron. J.* 96: 884
Thomas, P. 1989. *Ap. J.* In press
Tinsley, B. M. 1979. *Ap. J.* 229: 1046
Trumpler, R. J., Weaver, H. F. 1953. *Statistical Astronomy*. Berkeley: Univ. Calif. Press
Twarog, B. A. 1980. *Ap. J.* 242: 242
Upgren, A. R. Jr. 1962. *Astron. J.* 67: 37
Vanden Berg, D., Bell, R. A. 1985. *Ap. J. Suppl.* 58: 711
van den Bergh, S. 1958. *Astron. J.* 63: 492
van den Bergh, S. 1962. *Astron. J.* 67: 486
van den Bergh, S. 1979. In *Scientific Research With the Space Telescope. NASA CP-2111*, ed. M. S. Longair, J. W. Warner, p. 151
van den Bergh, S., McClure, R. D., Evans, R. 1987. *Ap. J.* 323: 44
van der Kruit, P. C., Freeman, K. C. 1986. *Ap. J.* 303: 556
van der Kruit, P. C., Searle, L. 1982. *Astron. Astrophys.* 110: 61
Weistrop, D. 1972. *Astron. J.* 77: 849
Wesselink, Th., Le Poole, R. S., Lub, J. 1987. In *Stellar Evolution and Dynamics in the Outer Halo of the Galaxy*, ed. M. Azzopardi, F. Matteucci, p. 185. Garching: ESO
Wheeler, J. C., Sneden, C., Truran, J. W. Jr. 1989. *Annu. Rev. Astron. Astrophys.* 27: 279
White, S. D. M. 1985. *Ap. J. Lett.* 294: L99
White, S. D. M. 1989a. In *The Epoch of Galaxy Formation. NATO Adv. Study Inst., Durham, Engl. 1988*, ed. R. Ellis, C. Frenk, J. Peacock. Dordrecht: Reidel. In press
White, S. D. M. 1989b. *MNRAS* 237: 41P
White, S. D. M., Rees, M. J. 1978. *MNRAS* 183: 341
Wielen, R. 1974. In *Highlights of Astronomy*, ed. G. Contopoulos, 3: 395. Dordrecht: Reidel
Woosley, S. E., Weaver, T. A. 1986. *Annu. Rev. Astron. Astrophys.* 24: 205
Wyse, R. F. G., Gilmore, G. 1986. *Astron. J.* 91: 855
Wyse, R. F. G., Gilmore, G. 1988. *Astron. J.* 95: 1404
Wyse, R. F. G., Gilmore, G. 1989. *Comments Astrophys.* 13: 135
Yoshii, Y. 1982. *Publ. Astron. Soc. Jpn.* 34: 365
Yoshii, Y. 1984. *Astron. J.* 89: 1190
Yoshii, Y., Ishida, K., Stobie, R. S. 1987. *Astron. J.* 93: 323
Yoshii, Y., Saio, H. 1979. *Publ. Astron. Soc. Jpn.* 31: 339
Yoss, K. M., Neese, C. L., Hartkopf, W. I. 1987. *Astron. J.* 94: 1600
Zinn, R. 1985. *Ap. J.* 293: 424
Zurek, W. H., Quinn, P. J., Salmon, J. K. 1988. *Ap. J.* 330: 519